

## DYNAMICAL ANALYSIS OF A PLANT–HERBIVORE MODEL WITH DOUBLE DELAY EFFECT AND DOUBLE ALLEE EFFECT

XIAOQUAN KONG, ZHENJIE ZHANG AND RUIZHI YANG\*

**Abstract.** In this study, a plant–herbivore model with double time delays and double Allee effects was constructed, incorporating intraspecific competition among herbivores. Theoretical analyses established the existence conditions of the positive equilibrium point and the boundedness of solutions. The stability and Hopf bifurcation of equilibria in the non-delayed system were thoroughly investigated, and the existence of Hopf bifurcations and global stability under double delays were examined. Numerical simulations demonstrated that when delays exceed critical thresholds, Hopf bifurcations occur, leading to system instability. Double Allee effects were shown to exacerbate this process, with increasing Allee intensity reducing plant population density.

**Mathematics Subject Classification.** 34K20, 34K18, 92D25.

Received May 31, 2025. Accepted February 19, 2026.

### 1. INTRODUCTION

Mathematical modeling provides a powerful theoretical framework for analyzing complex biological systems, with particular benefits in ecological dynamics research. Since Lotka and Volterra proposed the classic predator–prey model [1, 2], scholars have developed diverse theoretical frameworks to address the core ecological dynamics question of plant–herbivore interactions [3–7]. Recent studies increasingly demonstrate that the Allee effect, as a positive density-dependent feedback mechanism, holds special ecological significance in plant–herbivore systems.

The Allee Effect refers to the phenomenon where population growth rates decline when population density falls below a critical threshold. This concept was first introduced by American ecologist W.C.A in the 1930s [8]. The Allee effect can be categorized into two distinct types: the strong Allee effect and the weak Allee effect [9–11]. A strong Allee effect occurs when populations exhibit negative growth rates below a specific density threshold, inevitably leading to extinction. In contrast, the weak Allee effect describes populations maintaining positive growth rates at low densities but lacking a definitive extinction threshold. Notably, the double Allee effect has been demonstrated to significantly influence the state dynamics of interacting species in predator–prey systems. In their work, F. Wang *et al.* revealed through simulations that systems incorporating a double Allee effect exhibit substantially smaller stable regions and Turing instability regions compared to systems without this effect, indicating heightened sensitivity to parameter variations in most cases [12]. J. Jiao *et al.* demonstrated through the analysis of topologically equivalent normal systems that the Allee effect combined with time delays can induce distinct dynamic behaviors [13]. The mathematical formulation of growth functions

---

*Keywords and phrases:* Plant–herbivore, double Allee effect, double time delay, global stability, Hopf bifurcation.

Department of Mathematics, Northeast Forestry University Harbin 150040, Heilongjiang, China.

\* Corresponding author: [yangruizhi529@163.com](mailto:yangruizhi529@163.com)

for single species influenced by the double Allee effect was proposed in [14], expressed as follows

$$\frac{dP}{dt} = \frac{rP}{P+n_0} \left(1 - \frac{P}{K}\right) (P - m_0). \quad (1.1)$$

In this equation,  $P$  denotes the plant population density.  $K$  represents the environmental carrying capacity. Furthermore, the intrinsic growth rate of the species is influenced by two types of Allee effects. One is the linear factor  $m(P) = P - m_0$ , and the other is the hyperbolic function  $r(P) = \frac{rP}{P+n_0}$ . This model can be regarded as an approximate description of population dynamics without explicitly distinguishing between fertile and infertile individuals [15]. In the model, the parameter  $m_0$  represents the threshold of the Allee effect. When  $m_0 > 0$ , the population growth rate becomes negative when the population density falls below a certain threshold, leading to population extinction. This scenario is referred to as the strong Allee effect. When  $m_0 < 0$ , the population growth rate remains positive even when the population density is below a certain threshold, corresponding to the weak Allee effect. The auxiliary parameter  $n_0 > 0$  is used to quantify the intensity of another Allee effect caused by factors such as difficulties in finding mates, and it satisfies  $m_0 + n_0 > 0$ . The parameter  $n_0$  influences the overall shape of the average population growth curve. As  $n_0$  increases, the growth curve becomes flatter, and its maximum value correspondingly decreases [16].

While numerous studies have extensively investigated the role of single Allee effects in plant trophic levels, research on the mechanistic implications of double Allee effects within these systems remains relatively under-explored. Building upon the aforementioned analyses, this study focuses on the following plant–herbivore model incorporating a double Allee effect, aiming to elucidate its impacts on system stability and dynamic behaviors

$$\begin{cases} \frac{dP}{dt} = \frac{rP}{P+n_0} \left(1 - \frac{P}{K}\right) (P - m_0) - bPH, \\ \frac{dH}{dt} = cPH - dH - lH^2. \end{cases} \quad (1.2)$$

Where  $P(t)$  and  $H(t)$  denote the population densities of plants and herbivores at time  $t$ , respectively. The parameter  $b$  represents the capture rate, quantifying the rate at which herbivores consume the plant population. The conversion efficiency  $c$  describes the proportion of consumed plant biomass that is converted into herbivore biomass. The mortality rate  $d$  characterizes the natural death rate of the herbivore population, while  $l$  signifies the intraspecific competition coefficient, reflecting the intensity of competition among herbivores for limited resources.

In recent years, the role of time delays in ecosystem dynamics has received considerable attention [17–22]. For instance, Pal *et al.* [17] investigated a ratio-dependent model with a single delay and revealed the conditions for uniform persistence of the system under the combined effects of intraspecific competition and time delay. Enatsu *et al.* [18, 19] explored the impact of maturation delay and found that a prolonged maturation period of predators significantly increases their risk of extinction, and that the presence of time delay alters the bifurcation curves and thresholds observed in systems without delay. Upadhyay R K [20] analyzed an ecological model with two delays, revealing opposing roles of the carrying effect and fear effect in stability control. It was found that the carrying effect plays a dual role in both stabilizing and destabilizing the system, while the gestation delay consistently exhibits a destabilizing effect. Meanwhile, the combination of Allee effects and time delays in plant–herbivore models has begun to attract attention. Kumar and Verma [23, 24] introduced a single time delay into a Leslie–Gower model and a strong Allee effect model, respectively, and observed stability switches and Hopf bifurcations. However, the aforementioned studies are either confined to a single delay mechanism or fail to simultaneously consider double Allee effects.

Given the inherent time delays in biological processes, such as the time delay required for immature individuals to reach reproductive maturity [17–19], we incorporate a maturation delay  $\tau_1$  into the plant growth term of the Logistic equation to account for the physiological duration between resource assimilation and biomass accumulation in plants. Additionally, the gestation delay  $\tau_2$  representing the period between herbivore consumption and subsequent reproductive output is introduced to address the temporal decoupling of plant consumption and herbivore population growth driven by energy conversion [20–22]. While recent studies have predominantly

focused on single-delay mechanisms or isolated Allee effects, this work innovatively integrates double delay into a plant–herbivore model with double Allee effects, establishing the following system to systematically investigate their synergistic impacts

$$\begin{cases} \frac{dP}{dt} = \frac{rP}{P+n_0} \left(1 - \frac{P(t-\tau_1)}{K}\right) (P - m_0) - bPH, \\ \frac{dH}{dt} = cP(t - \tau_2)H(t - \tau_2) - dH - lH^2. \end{cases} \quad (1.3)$$

The aim of this study is to characterize the regulatory mechanisms of double time delay differences and double Allee effect strengths on nonlinear oscillations, stability changes, and population dynamics in plant–herbivore systems, quantify the time delay management windows and Allee effect intervention thresholds, and contribute to precise ecosystem regulation.

The structure of this paper is outlined as follows: In Section 2, we examined the existence and boundedness of the positive equilibrium, and analyzed its stability and Hopf bifurcation in both delayed and non-delayed systems. In Section 3, numerical simulations are conducted to demonstrate the theoretical findings. In Section 4, a brief conclusion is presented.

## 2. DYNAMIC OF NON-DELAYED MODEL

### 2.1. Existence of equilibrium points and boundedness of the solution

The non-delayed system (1.2) exhibits three biologically feasible equilibrium points:  $E_1(0, 0)$ ,  $E_2(K, 0)$ , and  $E_3(H^*, P^*)$ . While  $E_1$  and  $E_2$  are unconditionally present in the system, the coexistence equilibrium  $E_3$  holds particular ecological significance as it represents the sustainable state where both plant and herbivore populations coexist. Therefore, examining the existence and stability of the positive equilibrium  $E_3$  forms a pivotal component of this study. We rigorously examine the conditions governing the existence of this biologically meaningful equilibrium point.

**Theorem 2.1.** *The model has one positive equilibrium point if either of the following conditions is satisfied*

- (i)  $P^* > \frac{d}{c}$  and  $cm_0 < d < cK$ .
- (ii)  $P^* > \frac{d}{c}$ ,  $d = cm_0$  and  $n_0 < \frac{crKl+crm_0l-2lrd-cbKd}{bKc^2}$ .

*The model has two positive equilibrium points if either of the following conditions is satisfied*

- (iii)  $P^* > \frac{d}{c}$ ,  $d > \max\{cK, cm_0\}$  and  $\frac{lr(K+m_0)+2\sqrt{lm_0rK(bcK+lr)}}{bcK} \leq n_0 < \frac{crKl+crm_0l-2lrd-cbKd}{bKc^2}$ .
- (iv)  $P^* > \frac{d}{c}$ ,  $d > \max\{cK, cm_0\}$ ,  $n_0 < \frac{crKl+crm_0l-2lrd-cbKd}{bKc^2}$  and  $d > d_1$ .

*Proof.* From the non-delayed system (1.2), we can obtain

$$\begin{cases} \frac{rP}{P+n_0} \left(1 - \frac{P}{K}\right) (P - m_0) - bPH = 0, \\ cPH - dH - lH^2 = 0. \end{cases} \quad (2.1)$$

The second equation of system (2.1) yields the herbivore density  $H^* = \frac{cP^*-d}{l}$  which is biologically feasible only when  $P^* > \frac{d}{c}$  to ensure non-negative population values. Substituting this equilibrium herbivore density  $H^*$  back into the first equation of (2.1) generates a quadratic equation in the single variable  $P^*$

$$f(P^*) = AP^{*2} + BP^* + C \quad (2.2)$$

Let the coefficients be defined as:  $A = lr + cbK > 0$ ,  $B = bKcn_0 - lrK - lrm_0 - bKd$ ,  $C = Klr m_0 - bn_0dK$ . The system possesses a unique positive equilibrium point if either  $f(\frac{d}{c}) < 0$  holds, or both  $f(\frac{d}{c}) = 0$  and  $-\frac{B}{2A} > \frac{d}{c}$

are satisfied. When  $f(\frac{d}{c}) > 0$  and  $-\frac{B}{2A} > \frac{d}{c}$ , the discriminant of (2.2) can be written as a quadratic equation in the single variable  $d$

$$\Delta(d) = Hd^2 + Gd + F \quad (2.3)$$

where

$$\begin{aligned} H &= b^2 K^2 > 0, \\ G &= 2Kb(bcKn_0 + lr(K + m_0 + 2n_0)) > 0, \\ F &= b^2 c^2 K^2 n_0^2 - 2bcKlr(m_0 n_0 + K(2m_0 + n_0)) + l^2 r^2 (K - m_0)^2. \end{aligned}$$

It can be seen that the equation has at most one zero point, set as  $d_1$

$$\begin{aligned} d_1 &= \frac{1}{b^2 K^2} \left\{ -b^2 c K^2 n_0 - bKl(K + m_0 + 2n_0)r \right. \\ &\quad \left. + \sqrt{2} \sqrt{b^2 K^2 lr(K + n_0)(m_0 + n_0)(bcK + lr)} \right\} \end{aligned}$$

Case(i)  $\Delta(0) < 0, d > d_1$  or  $\Delta(0) \geq 0$  the system has two positive equilibrium point. Case(ii)  $\Delta(0) < 0, d = d_1$ , the system has one positive equilibrium point.  $\square$

**Theorem 2.2.** *The solutions of the non-delayed system (1.2) are uniformly bounded, satisfying  $0 \leq P(t) \leq M_1$  and  $0 \leq H(t) \leq M_2$ , where  $M_1 = K$  and  $M_2 = \frac{cK-d}{l}$ . This boundedness property ensures the biological validity of the model.*

*Proof.* From the first equation of model (1.2), we derive the following expression

$$\frac{dP}{dT} \leq \frac{rP(P - m_0)}{P + n_0} \left(1 - \frac{P}{k}\right) \leq \frac{rP^2}{P + n_0} \left(1 - \frac{P}{k}\right) \leq rP \left(1 - \frac{P}{k}\right)$$

By applying the standard comparison theorem, we can systematically derive the following conclusions

$$\limsup_{t \rightarrow \infty} P(t) \leq K$$

From the second equation of model (1.2), we get

$$\frac{dH}{dT} \leq H(cM_1 - d) - lH^2$$

Based on the comparison theorem, it can be readily deduced that

$$\limsup_{t \rightarrow \infty} H(t) \leq \frac{cK - d}{l}$$

$\square$

## 2.2. Local stability analysis and hopf bifurcation

For the convenience of calculation, record  $\bar{d} = \frac{d}{c}$ ,  $\bar{l} = \frac{l}{c}$ ,  $d$  and  $l$  are still used in the formula.

$$\begin{cases} \frac{dP}{dt} = \frac{rP}{P+n_0} \left(1 - \frac{P}{K}\right) (P - m_0) - bPH, \\ \frac{dH}{dt} = cH(P - d - lH). \end{cases} \quad (2.4)$$

The non-delayed model (2.1) possesses three equilibrium points:  $E_1(0, 0)$ ,  $E_2(K, 0)$  and  $E_3(H^*, P^*)$ . To analyze the stability of these equilibrium points, we first derive the Jacobian matrix of the non-delayed system

$$J_0(H, P) = \begin{pmatrix} a_{11} & a_{12} \\ a_{21} & a_{22} \end{pmatrix}. \quad (2.5)$$

where

$$a_{11} = \frac{-bHK(n_0 + P)^2 + (P(2m_0n_0 + m_0P - 3n_0P - 2P^2) + k(-m_0n_0 + 2n_0P + P^2))r}{K(n_0 + P)^2},$$

$$a_{12} = -bP < 0,$$

$$a_{21} = cH > 0,$$

$$a_{22} = cP - cd - 2lcH.$$

**Theorem 2.3.** *The boundary equilibrium point  $E_1(0, 0)$  of the system is a stable node.*

*Proof.* By evaluating the Jacobian matrix at the equilibrium point  $E_1$  we obtain

$$J_{E_1(0,0)} = \begin{pmatrix} \frac{-m_0r}{n_0} & 0 \\ 0 & -cd \end{pmatrix}.$$

□

By calculating the characteristic equation, the eigenvalue can be obtained as  $\lambda_1 = -\frac{m_0r}{n_0} < 0$  and  $\lambda_2 = -d < 0$ , thus  $E_1$  is a stable node.

**Theorem 2.4.** *If the boundary equilibrium point  $E_2(K, 0)$  of the system satisfies the following conditions*

(i) *if  $m < K < d$  it is a stable node.*

(ii) *if  $d < K < m$  it is an unstable node.*

(iii) *if  $K > \max\{d, m\}$  or  $K < \min\{d, m\}$  it is an unstable saddle point.*

*Proof.* By computing the Jacobian matrix at the equilibrium point  $E_2$  we obtain

$$J_{E_2(K,0)} = \begin{pmatrix} \frac{(-K+m)r}{K+n} & -bK \\ 0 & c(K-d) \end{pmatrix}.$$

□

By calculating the characteristic equation, the eigenvalue can be obtained as  $\lambda_1 = \frac{r(-K+m)}{K+n}$  and  $\lambda_2 = c(K-d)$ . Under condition (i), where  $\lambda_1 < 0$  and  $\lambda_2 < 0$ , the equilibrium point  $E_2$  is a stable node. Under condition (ii), where  $\lambda_1 > 0$  and  $\lambda_2 > 0$ ,  $E_2$  becomes an unstable node. Finally, under condition (iii),  $E_2$  is an unstable saddle point.

**Theorem 2.5.** *Consider the system with the following conditions*

$$d < \min \left\{ P^*, \frac{2bKP^* + 2lrP^* - Klr}{bK} \right\}, \quad c > U_1, \quad K < 2P^*.$$

*Under these conditions, the positive equilibrium  $E_3(P^*, H^*)$  is locally asymptotically stable. Furthermore, the quantity  $U_1$  is defined as*

$$U_1 = \frac{1}{lH^*K(n_0 + P^*)^2} \left\{ -bH^*K(n_0 + P^*)^2 + r \left( P^*(2m_0n_0 + m_0P^* - 3n_0P^* - 2(P^*)^2) + K(-m_0n_0 + 2n_0P^* + (P^*)^2) \right) \right\}$$

*Proof.* By evaluating the Jacobian matrix at the equilibrium point  $E_3$  we obtain

$$J_{E_3(H^*, P^*)} = \begin{pmatrix} \frac{-bH^*K(n_0+P^*)^2 + (P^*(2m_0n_0+m_0P^*-3n_0P^*-2(P^*)^2) + K(-m_0n_0+2n_0P^+(P^*)^2))r}{K(n_0+P^*)^2} & -bP^* \\ cH^* & -lcH^* \end{pmatrix}.$$

Through calculations, the characteristic equation is given by

$$\lambda^2 - B\lambda + T = 0. \quad (2.6)$$

among

$$\begin{aligned} B &= lH^*(U_1 - c) \\ T &= \frac{1}{Kl(n_0 + p^*)^2} \left\{ c(d - p^*) (bK(d - 2p^*)(n_0 + p^*)^2 + lr(p^*(2m_0n_0 + m_0p^* - 3n_0p^* - 2(p^*)^2) + K(-m_0n_0 + 2n_0p^* + (p^*)^2))) \right\} \end{aligned}$$

Through simplification we can get

$$\begin{aligned} T &= \frac{1}{Kl(n_0 + p^*)^2} \left\{ c(d - p^*) (bK(d - 2p^*)(n_0 + p^*)^2 + lr(p^*(2m_0n_0 + m_0p^* - 3n_0p^* - 2(p^*)^2) + K(-m_0n_0 + 2n_0p^* + (p^*)^2))) \right\} \\ &= \frac{1}{Kl(n_0 + p^*)^2} \left\{ c(d - p^*)(n_0 + p^*)^2 (bK(d - 2p^*) - 2lrp^* + Klr) + lr(p^*(2m_0n_0 + m_0p^* + 2n_0^2 + n_0p^*) + K(-m_0n_0 - n_0^2)) \right\} \\ &= \frac{1}{Kl(n_0 + p^*)^2} \left\{ c(d - p^*)(n_0 + p^*)^2 (bk(d - 2p^*) - 2lrp^* + Klr) + lr(p^*(m_0p^* + n_0p^*) + (m_0n_0 + n_0^2)(2p^* - K)) \right\} \end{aligned}$$

□

So, when  $d < \min \left\{ P^*, \frac{2bKP^* + 2lrP^* - Klr}{bK} \right\}, c > U_1, K < 2P^*$ , we can drive that  $T > 0$  and  $B < 0$ . Consequently, the positive equilibrium is locally asymptotically stable.

When  $B = 0$ , the characteristic equation (2.6) necessarily possesses a pair of purely imaginary conjugate roots, satisfying the critical criterion for Hopf bifurcation. Since  $B$  explicitly depends on the parameter  $c$ , this parameter serves as a viable candidate for triggering the bifurcation. To maintain generality in the analysis,  $c$  is

selected as the bifurcation parameter. To rigorously establish the transversality condition for Hopf bifurcation, we compute the derivative of  $B$  with respect to  $c$ , yielding

$$\frac{dB}{dc} = -lH^* < 0$$

So, it can be said that the parameter  $c$  acts as a Hopf-bifurcation parameter.

### 2.3. Global stability analysis

**Theorem 2.6.** *The positive equilibrium  $E_3(H^*, P^*)$  of the system (1.2) is globally asymptotically stable provided the following criteria, denoted by  $(W_1)$ , are satisfied*

- (i)  $P^* > \frac{d}{c}$  and  $cm_0 < d < cK$ ;
- (ii)  $d < \min \left\{ P^*, \frac{2bKP^* + 2lrP^* - Klr}{bK} \right\}$ ,  $c > U_1$ ,  $K < 2P^*$ ;
- (iii)  $c < \min \left\{ \frac{3r}{K}, \frac{dK - 2(K+m_0)r}{Kn_0} \right\}$ .

*Proof.* For the dynamical system described in equation (1.2) we construct the Dulac function  $\phi(P, H)$  as:  $\phi(P, H) = P + n_0$ . Through detailed calculations, we obtain the following results

$$\begin{aligned} \Gamma(P, H) &= \frac{\partial}{\partial P} \left( \phi \frac{dP}{dt} \right) + \frac{\partial}{\partial H} \left( \phi \frac{dH}{dt} \right) \\ &= \frac{\partial}{\partial P} \left( -\frac{P(bHK(n_0 + P) + (K - P)(m_0 - P)r)}{K} \right) \\ &\quad + \frac{\partial}{\partial H} (-H(n_0 + P)(d + Hl - cP)) \\ &= \left( c - \frac{3r}{K} \right) P^2 + \left( 2r - d + cn_0 + \frac{2m_0r}{K} \right) P \\ &\quad - (m_0r + dn_0 + H(2ln_0 + 2lP + b(n_0 + 2P))) \end{aligned}$$

Therefore, when  $c < \min \left\{ \frac{3r}{K}, \frac{dK - 2(K+m_0)r}{Kn_0} \right\}$ , we have  $\Gamma(P, H) < 0$ . Consequently, by the Bendixson-Dulac theorem [25], it follows that the system admits no closed orbits within the positive quadrant  $D = \{(P, H) : P > 0, H > 0\}$ , thereby ruling out the existence of periodic solutions. Simultaneously, conditions (i) and (ii) guarantee the existence of a unique positive equilibrium point, which is locally asymptotically stable. Consequently, the system possesses a unique globally asymptotically stable equilibrium point within the positive quadrant, and all solutions converge to this equilibrium.  $\square$

## 3. DYNAMICS OF THE DELAYED MODEL

### 3.1. Local stability analysis

To incorporate biological realism into the model, we introduce two distinct time delays: a maturation delay  $\tau_1$  and a gestation delay  $\tau_2$ . These delays are integrated into system (1.2), which is then linearized around the positive equilibrium point to analyze its local dynamical behavior. The Jacobian matrix of system (1.3) is calculated at the equilibrium point  $E_3(H^*, P^*)$  as follows

$$A = \begin{pmatrix} m_{11} + n_{11}e^{-\lambda\tau_1} & m_{12} \\ n_{21}e^{-\lambda\tau_2} & m_{22} + n_{22}e^{-\lambda\tau_2} \end{pmatrix}$$

where

$$\begin{aligned} m_{11} &= \frac{1}{k(n_0 + P^*)^2} \left( (2rP^* - rm_0)(P^* + n_0) - (rP^{*2} - rP^*m_0) \right) (k - P^*) - bH^*, \\ m_{12} &= -bP^*, \quad m_{22} = -d - 2lH^*, \quad n_{11} = \frac{rP^*(m_0 - P^*)}{K(n_0 + P^*)}, \\ n_{21} &= cH^*, \quad n_{22} = cP^*. \end{aligned}$$

The characteristic equation for system (1.3) can be expressed as follows

$$\begin{aligned} \lambda^2 + (-m_{11} - m_{22})\lambda + (n_{11}m_{22} - n_{11}\lambda)e^{-\lambda\tau_1} + (m_{11}n_{22} - m_{12}n_{21} - n_{22}\lambda)e^{-\lambda\tau_2} \\ + n_{11}n_{22}e^{-\lambda(\tau_2+\tau_1)} + m_{11}m_{22} = 0. \end{aligned} \quad (3.1)$$

In the subsequent analysis, the local stability properties of system (1.3) will be systematically examined from four distinct perspectives.

### 3.1.1. Case with only maturation delay ( $\tau_1 > 0$ , $\tau_2 = 0$ )

The characteristic equation (3.1) transforms into the following form

$$\lambda^2 + H_1\lambda + H_2 + (G - n_{11}\lambda)e^{-\lambda\tau_1} = 0 \quad (3.2)$$

where

$$H_1 = -m_{11} - m_{22} - n_{22}, H_2 = m_{11}m_{22} - m_{12}n_{21} + m_{11}n_{22}, G = n_{11}m_{22} + n_{11}n_{22}.$$

Assuming that  $\lambda = i\omega_1$ , where  $\omega_1 > 0$ , is a root of equation (3.2), we substitute this into equation (3.2) to obtain

$$-\omega_1^2 + i\omega_1 H_1 + H_2 + (G - n_{11}i\omega_1)e^{-i\omega_1\tau_1} = 0$$

By separating the real and imaginary parts, we obtain the following expressions

$$\omega_1^2 - H_2 = G \cos(\omega_1\tau_1) - n_{11}\omega_1 \sin(\omega_1\tau_1) \quad (3.3)$$

$$\omega_1 H_1 = G \sin(\omega_1\tau_1) + n_{11}\omega_1 \cos(\omega_1\tau_1) \quad (3.4)$$

We can obtain  $\sin(\omega_1\tau_1) = \frac{GH_1\omega_1 + H_2n_{11}\omega_1 - n_{11}\omega_1^3}{G^2 + n_{11}^2\omega_1^2}$  and  $\cos(\omega_1\tau_1) = \frac{-GH_2 + G\omega_1^2 + H_1n_{11}\omega_1^2}{G^2 + n_{11}^2\omega_1^2}$ . By squaring equations (3.3) and (3.4) individually and summing the results, we derive the following quartic equation in a single variable

$$\omega_1^4 + P_1\omega_1^2 + P_2 = 0 \quad (3.5)$$

where

$$P_1 = H_1^2 - 2H_2 - n_{11}^2, P_2 = H_2^2 - G^2.$$

If the condition (S1)  $P_2 < 0$  is satisfied, which is equivalent to  $H_2^2 < G^2$ , then equation (3.5) admits a positive root. Assuming  $\omega_1^0$  is the unique positive root of equation (3.5), substituting  $\omega_1^0$  into equations (3.3) and (3.4) yields

$$\tau_1^n = \frac{1}{\omega_1^0} \arccos \left[ \frac{-GH_2 + G(\omega_1^0)^2 + H_1 n_{11} (\omega_1^0)^2}{G^2 + n_{11}^2 (\omega_1^0)^2} \right] + \frac{2n\pi}{\omega_1^0}, n = 0, 1, 2, \dots$$

For any  $\epsilon > 0$ , let  $\lambda(\tau_1) = \beta_1(\tau_1) + i\eta_1(\tau_1)$  be a root of the characteristic equation within the  $\epsilon$  neighborhood of  $\tau_1^n$ , satisfying  $\beta_1(\tau_1^n) = 0$  and  $\eta_1(\tau_1^n) = \omega_1^0$ . Substituting  $\lambda(\tau_1)$  into the left-hand side of equation (3.2) and differentiating with respect to  $\tau_1$ , we derive

$$\left( \frac{d\lambda}{d\tau_1} \right)^{-1} = \frac{(2\lambda + H_1)e^{\lambda\tau_1} - n_{11}}{\lambda(G - n_{11}\lambda)} - \frac{\tau_1}{\lambda}$$

Based on the above analysis, we can further obtain the following equation

$$\begin{aligned} \text{sign} \left\{ \frac{d(\text{Re}\lambda)}{d\tau_1} \right\}_{\lambda=i\omega_1^0} &= \text{sign} \left\{ \text{Re} \left( \frac{d\lambda}{d\tau_1} \right)^{-1} \right\}_{\lambda=i\omega_1^0} \\ &= \text{sign} \left\{ \frac{1}{-(\omega_1^0)^2 G^2 - n_{11}^2 (\omega_1^0)^4} \left( (-2(\omega_1^0)^2 G - n_{11} (\omega_1^0)^2 H_1) \cos(\omega_1^0 \tau_1) \right. \right. \\ &\quad \left. \left. + (2n_{11} (\omega_1^0)^3 - H_1 G \omega_1^0) \sin(\omega_1^0 \tau_1) + n_{11}^2 (\omega_1^0)^2 \right) \right\} \\ &= \text{sign} \left\{ \frac{H_1^2 - 2H_2 - n_{11}^2 + 2(\omega_1^0)^2}{G^2 + n_{11}^2 (\omega_1^0)^2} \right\} \end{aligned}$$

If the inequality (S2)  $H_1^2 + 2(\omega_1^0)^2 > 2H_2 + n_{11}^2$  holds, it follows that  $\text{sign} \left\{ \frac{d(\text{Re}\lambda)}{d\tau_1} \right\}_{\lambda=i\omega_1^0} > 0$ , consequently,  $\left[ \frac{d(\text{Re}\lambda)}{d\tau_1} \right]_{\tau=\tau_1^0} > 0$ . This provides a sufficient condition under which at least one eigenvalue with a positive real part emerges when  $\tau > \tau_1^0$ .

**Theorem 3.1.** *Under the conditions  $\tau_1 > 0$  and  $\tau_2 = 0$ , if conditions (S1) and (S2) are both satisfied, we have the following conclusions.*

- (i) *When  $\tau_1 \in [0, \tau_1^0)$ , the equilibrium point  $E_3(H^*, P^*)$  is locally asymptotically stable.*
- (ii) *When  $\tau_1 > \tau_1^0$ , the system becomes unstable at the equilibrium point  $E_3(H^*, P^*)$ .*
- (iii) *When  $\tau_1 = \tau_1^n$ , a Hopf bifurcation occurs in the system near the equilibrium  $E_3(H^*, P^*)$ .*

### 3.1.2. Case with only gestation delay ( $\tau_1 = 0, \tau_2 > 0$ )

The characteristic equation (3.1) transforms into the following form

$$\lambda^2 + Q_1\lambda + Q_2 + (R - n_{22}\lambda)e^{-\lambda\tau_2} = 0 \tag{3.6}$$

where

$$Q_1 = -m_{11} - m_{22} - n_{11}, Q_2 = n_{11}m_{22} + m_{11}m_{22}, R = m_{11}n_{22} - m_{12}n_{21} + n_{11}n_{22}.$$

Assuming that  $\lambda = i\omega_2$ , where  $\omega_2 > 0$ , is a root of equation (3.6), we substitute this into equation (3.6) to obtain

$$-\omega_2^2 + i\omega_2 Q_1 + Q_2 + (R - n_{22}i\omega_2)e^{-i\omega_2\tau_2} = 0$$

By separating the real and imaginary parts, we obtain the following expressions

$$\omega_2^2 - Q_2 = R \cos(\omega_2 \tau_2) - n_{22} \omega_2 \sin(\omega_2 \tau_2) \quad (3.7)$$

$$\omega_2 Q_1 = R \sin(\omega_2 \tau_2) + n_{22} \omega_2 \cos(\omega_2 \tau_2) \quad (3.8)$$

We can obtain  $\sin(\omega_2 \tau_2) = \frac{RQ_1\omega_2 + Q_2 n_{22} \omega_2 - n_{22} \omega_2^3}{R^2 + n_{22}^2 \omega_2^2}$  and  $\cos(\omega_2 \tau_2) = \frac{-RQ_2 + R\omega_2^2 + Q_1 n_{22} \omega_2^2}{R^2 + n_{22}^2 \omega_2^2}$ . By squaring equations (3.7) and (3.8) individually and summing the results, we derive the following quartic equation in a single variable

$$\omega_2^4 + L_1 \omega_2^2 + L_2 = 0 \quad (3.9)$$

where

$$L_1 = Q_1^2 - 2Q_2 - n_{22}^2, L_2 = Q_2^2 - R^2.$$

If the condition (S3)  $L_2 < 0$  is satisfied, which is equivalent to  $Q_2^2 < R^2$ , then equation (3.9) admits a positive root. Assuming  $\omega_2^0$  is the unique positive root of equation (3.9), substituting  $\omega_2^0$  into equations (3.7) and (3.8) yields

$$\tau_2^n = \frac{1}{\omega_2^0} \arccos \left[ \frac{-RQ_2 + R(\omega_2^0)^2 + Q_1 n_{22} (\omega_2^0)^2}{R^2 + n_{22}^2 (\omega_2^0)^2} \right] + \frac{2n\pi}{\omega_2^0}, n = 0, 1, 2, \dots$$

For any  $\epsilon > 0$ , let  $\lambda(\tau_2) = \beta_2(\tau_2) + i\eta_2(\tau_2)$  be a root of the characteristic equation within the  $\epsilon$  neighborhood of  $\tau_2^n$ , satisfying  $\beta_2(\tau_2^n) = 0$  and  $\eta_2(\tau_2^n) = \omega_2^0$ . Substituting  $\lambda(\tau_2)$  into the left-hand side of equation (3.6) and differentiating with respect to  $\tau_2$ , we derive

$$\left( \frac{d\lambda}{d\tau_2} \right)^{-1} = \frac{(2\lambda + Q_1)e^{\lambda\tau_2} - n_{22}}{\lambda(R - n_{22}\lambda)} - \frac{\tau_2}{\lambda}$$

Based on the above analysis, we can further obtain the following equation

$$\begin{aligned} \text{sign} \left\{ \frac{d(\text{Re}\lambda)}{d\tau_2} \right\}_{\lambda=i\omega_2^0} &= \text{sign} \left\{ \text{Re} \left( \frac{d\lambda}{d\tau_2} \right)^{-1} \right\}_{\lambda=i\omega_2^0} \\ &= \text{sign} \left\{ \frac{1}{-(\omega_2^0)^2 R^2 - n_{22}^2 (\omega_2^0)^4} \left( (-2(\omega_2^0)^2 R - n_{22} (\omega_2^0)^2 Q_1) \cos(\omega_2^0 \tau_2) \right. \right. \\ &\quad \left. \left. + (2n_{22} (\omega_2^0)^3 - Q_1 R \omega_2^0) \sin(\omega_2^0 \tau_2) + n_{22}^2 (\omega_2^0)^2 \right) \right\} \\ &= \text{sign} \left\{ \frac{Q_1^2 - 2Q_2 - n_{22}^2 + 2(\omega_2^0)^2}{R^2 + n_{22}^2 (\omega_2^0)^2} \right\} \end{aligned}$$

If the inequality (S4)  $Q_1^2 + 2(\omega_2^0)^2 > 2Q_2 + n_{22}^2$  holds, it follows that  $\text{sign} \left\{ \frac{d(\text{Re}\lambda)}{d\tau_2} \right\}_{\lambda=i\omega_2^0} > 0$ , consequently,  $\left[ \frac{d(\text{Re}\lambda)}{d\tau_2} \right]_{\tau=\tau_2^0} > 0$ . This provides a sufficient condition under which at least one eigenvalue with a positive real part emerges when  $\tau > \tau_2^0$ .

**Theorem 3.2.** *Under the conditions  $\tau_1 = 0$  and  $\tau_2 > 0$ , if conditions (S3) and (S4) are both satisfied, we have the following conclusions.*

- (i) When  $\tau_2 \in [0, \tau_2^0)$ , the equilibrium point  $E_3(H^*, P^*)$  is locally asymptotically stable.  
(ii) When  $\tau_2 > \tau_2^0$ , the system becomes unstable at the equilibrium point  $E_3(H^*, P^*)$ .  
(iii) When  $\tau_2 = \tau_2^0$ , a Hopf bifurcation occurs in the system near the equilibrium  $E_3(H^*, P^*)$ .

### 3.1.3. Case with both maturation delay and gestation delay ( $\tau_1 > 0$ , $\tau_2 \in [0, \tau_2^0)$ )

The characteristic equation (3.1) transforms into the following form

$$\lambda^2 + A\lambda + (B - C\lambda)e^{-\lambda\tau_1} + (D - E\lambda)e^{-\lambda\tau_2} + Fe^{-\lambda(\tau_1+\tau_2)} + G = 0 \quad (3.10)$$

where

$$A = -m_{11} - m_{22}, B = n_{11}m_{22}, C = n_{11},$$

$$D = m_{11}n_{22} - m_{12}n_{21}, E = n_{22}, F = n_{11}n_{22}, G = m_{11}m_{22}.$$

Assuming that  $\lambda = i\omega_3$ , where  $\omega_3 > 0$ , is a root of equation (3.10), we substitute this into equation (3.10). By separating the real and imaginary parts, we obtain the following expressions

$$M_1 \cos(\omega_3\tau_1) - N_1 \sin(\omega_3\tau_1) = Q_1 \quad (3.11)$$

$$M_1 \cos(\omega_3\tau_1) + N_1 \sin(\omega_3\tau_1) = Q_2 \quad (3.12)$$

where

$$M_1 = B + F \cos(\omega_3\tau_2), N_1 = C\omega_3 + F \sin(\omega_3\tau_2),$$

$$Q_1 = (\omega_3^2 - G) + E\omega_3 \sin(\omega_3\tau_2) - D \cos(\omega_3\tau_2),$$

$$Q_2 = -D \sin(\omega_3\tau_2) + A\omega_3 - E\omega_3 \cos(\omega_3\tau_2).$$

We can obtain  $\sin(\omega_3\tau_1) = \frac{M_1Q_2 - N_1Q_1}{M_1^2 + N_1^2}$  and  $\cos(\omega_3\tau_1) = \frac{M_1Q_1 + N_1Q_2}{M_1^2 + N_1^2}$ . By squaring equations (3.11) and (3.12) individually and summing the results, we derive the following quartic equation in a single variable

$$\omega_3^4 + a_1\omega_3^3 + a_2\omega_3^2 + a_3\omega_3 + a_4 = 0 \quad (3.13)$$

where

$$a_1 = 2E \sin(\omega_3\tau_2),$$

$$a_2 = A^2 + E^2 - C^2 - 2G + (-2D - 2AE) \cos(\omega_3\tau_2),$$

$$a_3 = -2 \sin(\omega_3\tau_2)(AD + CF + EG),$$

$$a_4 = G^2 + D^2 + 2DG \cos(\omega_3\tau_2) - (B + F \cos(\omega_3\tau_2))^2 - F^2 \sin^2(\omega_3\tau_2).$$

If the condition (S5)  $a_1 < 0$  is satisfied, which is equivalent to  $E \sin(\omega_3 \tau_2) < 0$ , then equation (3.13) admits a positive root. Assuming  $\omega_3^0$  is the unique positive root of equation (3.13), substituting  $\omega_3^0$  into equations (3.11) and (3.12) yields

$$\tau_{1*}^n = \frac{1}{\omega_3^0} \arccos \left[ \frac{M_1 Q_1 + N_1 Q_2}{M_1^2 + N_1^2} \right] + \frac{2n\pi}{\omega_3^0}, n = 0, 1, 2, \dots$$

For any  $\epsilon > 0$ , let  $\lambda(\tau_3) = \beta_3(\tau_3) + i\eta_3(\tau_3)$  be a root of the characteristic equation within the  $\epsilon$  neighborhood of  $\tau_3^n$ , satisfying  $\beta_3(\tau_3^n) = 0$  and  $\eta_3(\tau_3^n) = \omega_3^0$ . Substituting  $\lambda(\tau_3)$  into the left-hand side of equation (3.11) and differentiating with respect to  $\tau_3$ , we derive

$$\left( \frac{d\lambda}{d\tau_1} \right)^{-1} = \frac{(2\lambda + A)e^{\lambda(\tau_1 + \tau_2)} - Ce^{\lambda\tau_2} + e^{\lambda\tau_1}(-E - \tau_2(D - E\lambda)) - \tau_2 F}{\lambda((B - C\lambda)e^{\lambda\tau_2} + F)} - \frac{\tau_1}{\lambda}$$

Based on the above analysis, we can further obtain the following equation

$$\begin{aligned} \text{sign} \left\{ \frac{d(Re\lambda)}{d\tau_1} \right\}_{\lambda=i\omega_3^0} &= \text{sign} \left\{ Re \left( \frac{d\lambda}{d\tau_1} \right)^{-1} \right\}_{\lambda=i\omega_3^0} \\ &= \text{sign} \left\{ \frac{R_1(\omega_3^0)^3 + R_2(\omega_3^0)^2 + R_3\omega_3^0}{(R_4)^2 + (R_5)^2} \right\} \end{aligned}$$

where

$$R_1 = - (2C \sin(\omega_3^0 \tau_1) + CE\tau_2 \sin((\tau_1 - \tau_2)\omega_3^0)),$$

$$\begin{aligned} R_2 = & - (C^2 + (-2B - AC - EF\tau_2) \cos(\omega_3^0 \tau_1) + (CE + CD\tau_2 - BE\tau_2) \cos((\tau_1 - \tau_2)\omega_3^0) \\ & + CF\tau_2 \cos(\omega_3^0 \tau_2) - 2F \cos((\tau_1 + \tau_2)\omega_3^0)), \end{aligned}$$

$$\begin{aligned} R_3 = & (AB - F(E + D\tau_2)) \sin(\omega_3^0 \tau_1) - B(E + D\tau_2) \sin((\tau_1 - \tau_2)\omega_3^0) \\ & F((-C + B\tau_2) \sin(\omega_3^0 \tau_2) + A \sin((\tau_1 + \tau_2)\omega_3^0)), \end{aligned}$$

$$R_4 = C(\omega_3^0)^2 \cos(\omega_3^0 \tau_2) - B\omega_3^0 \sin(\omega_3^0 \tau_2),$$

$$R_5 = F\omega_3^0 + B\omega_3^0 \cos(\omega_3^0 \tau_2) + C(\omega_3^0)^2 \sin(\omega_3^0 \tau_2).$$

If the inequality (S6)  $R_1(\omega_3^0)^3 + R_2(\omega_3^0)^2 + R_3\omega_3^0 \neq 0$  holds, it follows that  $\text{sign} \left\{ \frac{d(Re\lambda)}{d\tau_1} \right\}_{\lambda=i\omega_3^0} \neq 0$ , consequently,  $\left[ \frac{d(Re\lambda)}{d\tau_1} \right]_{\tau=\tau_{1*}^0} \neq 0$ . This provides a sufficient condition under which at least one eigenvalue with a positive real part emerges when  $\tau > \tau_{1*}^0$ .

**Theorem 3.3.** *Under the conditions  $\tau_1 > 0$  and  $\tau_2 \in [0, \tau_2^0)$ , if conditions (S5) and (S6) are both satisfied, we have the following conclusions.*

- (i) *When  $\tau_1 \in [0, \tau_{1*}^0)$ , the equilibrium point  $E_3(H^*, P^*)$  is locally asymptotically stable.*
- (ii) *When  $\tau_1 > \tau_{1*}^0$ , the system becomes unstable at the equilibrium point  $E_3(H^*, P^*)$ .*
- (iii) *When  $\tau_1 = \tau_{1*}^0$ , a Hopf bifurcation occurs in the system near the equilibrium  $E_3(H^*, P^*)$ .*

3.1.4. *Case with both maturation delay and gestation delay* ( $\tau_2 > 0$ ,  $\tau_1 \in [0, \tau_1^0)$ )

The characteristic equation (3.1) transforms into the following form

$$\lambda^2 + A\lambda + (B - C\lambda)e^{-\lambda\tau_1} + (D - E\lambda)e^{-\lambda\tau_2} + Fe^{-\lambda(\tau_1+\tau_2)} + G = 0 \quad (3.14)$$

where

$$A = -m_{11} - m_{22}, B = n_{11}m_{22}, C = n_{11},$$

$$D = m_{11}n_{22} - m_{12}n_{21}, E = n_{22}, F = n_{11}n_{22}, G = m_{11}m_{22}.$$

Assuming that  $\lambda = i\omega_4$ , where  $\omega_4 > 0$ , is a root of equation (3.14), we substitute this into equation (3.14). By separating the real and imaginary parts, we obtain the following expressions

$$M_2 \cos(\omega_4\tau_2) - N_2 \sin(\omega_4\tau_2) = P_1 \quad (3.15)$$

$$N_2 \cos(\omega_4\tau_2) + M_2 \sin(\omega_4\tau_2) = P_2 \quad (3.16)$$

where

$$M_2 = D + F \cos(\omega_4\tau_1), N_2 = E\omega_4 + F \sin(\omega_4\tau_1),$$

$$P_1 = (\omega_4^2 - G) + C\omega_4 \sin(\omega_4\tau_1) - B \cos(\omega_4\tau_1),$$

$$P_2 = -B \sin(\omega_4\tau_1) + A\omega_4 - C\omega_4 \cos(\omega_4\tau_1).$$

We can obtain  $\sin(\omega_4\tau_2) = \frac{M_2P_2 - N_2P_1}{M_2^2 + N_2^2}$  and  $\cos(\omega_4\tau_2) = \frac{M_2P_1 + N_2P_2}{M_2^2 + N_2^2}$ . By squaring equations (3.15) and (3.16) individually and summing the results, we derive the following quartic equation in a single variable

$$\omega_4^4 + b_1\omega_4^3 + b_2\omega_4^2 + b_3\omega_4 + b_4 = 0 \quad (3.17)$$

where

$$b_1 = 2C \sin(\omega_4\tau_1),$$

$$b_2 = A^2 + C^2 - E^2 - 2G + (-2B - 2AC) \cos(\omega_4\tau_1),$$

$$b_3 = -2 \sin(\omega_4\tau_1)(AB + EF + CG),$$

$$b_4 = G^2 + B^2 + 2BG \cos(\omega_4\tau_1) - (D + F \cos(\omega_4\tau_1))^2 - F^2 \sin^2(\omega_4\tau_1).$$

If the condition (S7)  $b_1 < 0$  is satisfied, which is equivalent to  $C \sin(\omega_4\tau_1) < 0$ , then equation (3.17) admits a positive root. Assuming  $\omega_4^0$  is the unique positive root of equation (3.17), substituting  $\omega_4^0$  into equations (3.15)

and (3.16) yields

$$\tau_{2*}^n = \frac{1}{\omega_4^0} \arccos \left[ \frac{M_2 P_1 + N_2 P_2}{M_2^2 + N_2^2} \right] + \frac{2n\pi}{\omega_4^0}, n = 0, 1, 2, \dots$$

For any  $\epsilon > 0$ , let  $\lambda(\tau_4) = \beta_4(\tau_4) + i\eta_4(\tau_4)$  be a root of the characteristic equation within the  $\epsilon$  neighborhood of  $\tau_4^n$ , satisfying  $\beta_4(\tau_4^n) = 0$  and  $\eta_4(\tau_4^n) = \omega_4^0$ . Substituting  $\lambda(\tau_4)$  into the left-hand side of equation (3.14) and differentiating with respect to  $\tau_4$ , we derive

$$\left( \frac{d\lambda}{d\tau_2} \right)^{-1} = \frac{(2\lambda + Q_1)e^{\lambda\tau_2} - n_{22}}{\lambda(R - n_{22}\lambda)} - \frac{\tau_2}{\lambda}$$

Based on the above analysis, we can further obtain the following equation

$$\begin{aligned} \text{sign} \left\{ \frac{d(\text{Re}\lambda)}{d\tau_2} \right\}_{\lambda=i\omega_3^0} &= \text{sign} \left\{ \text{Re} \left( \frac{d\lambda}{d\tau_2} \right)^{-1} \right\}_{\lambda=i\omega_3^0} \\ &= \text{sign} \left\{ \frac{X_1(\omega_4^0)^3 + X_2(\omega_4^0)^2 + X_3\omega_4^0}{(X_4)^2 + (X_5)^2} \right\} \end{aligned}$$

where

$$X_1 = CE\tau_1 \sin((\tau_1 - \tau_2)\omega_4^0) - 2E \sin(\omega_4^0\tau_2),$$

$$\begin{aligned} X_2 &= -E^2 - EF\tau_1 \cos(\omega_4^0\tau_1) + (-CE + CD\tau_1 - BE\tau_1) \cos((\tau_1 - \tau_2)\omega_4^0) \\ &\quad + (2D + AE + CF\tau_1) \cos(\omega_4^0\tau_2) + 2F \cos((\tau_1 + \tau_2)\omega_4^0), \end{aligned}$$

$$\begin{aligned} X_3 &= (-EF + DF\tau_1) \sin(\omega_4^0\tau_1) + D(C + B\tau_1) \sin((\tau_1 - \tau_2)\omega_4^0) \\ &\quad + (AD - CF - BF\tau_1) \sin(\omega_4^0\tau_2) + AF \sin((\tau_1 + \tau_2)\omega_4^0), \end{aligned}$$

$$X_4 = E(\omega_4^0)^2 \cos(\omega_4^0\tau_1) - D\omega_4^0 \sin(\omega_4^0\tau_1),$$

$$X_5 = F\omega_4^0 + D\omega_4^0 \cos(\omega_4^0\tau_1) + E(\omega_4^0)^2 \sin(\omega_4^0\tau_1).$$

If the inequality (S8)  $X_1(\omega_4^0)^3 + X_2(\omega_4^0)^2 + X_3\omega_4^0 \neq 0$  holds, it follows that  $\text{sign} \left\{ \frac{d(\text{Re}\lambda)}{d\tau_2} \right\}_{\lambda=i\omega_4^0} \neq 0$ , consequently,  $\left[ \frac{d(\text{Re}\lambda)}{d\tau_2} \right]_{\tau=\tau_{2*}^0} \neq 0$ . This provides a sufficient condition under which at least one eigenvalue with a positive real part emerges when  $\tau > \tau_{2*}^0$ .

**Theorem 3.4.** *Under the conditions  $\tau_2 > 0$  and  $\tau_1 \in [0, \tau_1^0)$ , if conditions (S7) and (S8) are both satisfied, we have the following conclusions.*

- (i) *When  $\tau_2 \in [0, \tau_{2*}^0)$ , the equilibrium point  $E_3(H^*, P^*)$  is locally asymptotically stable.*
- (ii) *When  $\tau_2 > \tau_{2*}^0$ , the system becomes unstable at the equilibrium point  $E_3(H^*, P^*)$ .*
- (iii) *When  $\tau_2 = \tau_{2*}^0$ , a Hopf bifurcation occurs in the system near the equilibrium  $E_3(H^*, P^*)$ .*

### 3.2. Global asymptotic stability for the delayed system

#### 3.2.1. Case with only maturation delay ( $\tau_1 > 0$ , $\tau_2 = 0$ )

**Theorem 3.5.** *When  $\tau_1 > 0$  and  $\tau_2 = 0$ , under condition  $(W_1)$  in Theorem 2.6, the positive equilibrium point of system (1.3) is globally asymptotically stable[26].*

*Proof.* Define Lyapunov function  $V_1 = P - P^* - P^* \ln\left(\frac{P}{P^*}\right) + \gamma_1\left(H - H^* - H^* \ln\frac{H}{H^*}\right)$  and  $\gamma_1$  is a normal number greater than zero. Differentiating the given expression yields

$$\begin{aligned}
\frac{dV_1}{dT} &= \left(1 - \frac{P^*}{P}\right) \frac{dP}{dT} + \gamma_1 \left(1 - \frac{H^*}{H}\right) \frac{dH}{dT} \\
&= (P - P^*) \left[ \frac{r(P - m_0)}{P + n_0} - \frac{r(P - m_0)}{P + n_0} \frac{P(t - \tau_1)}{K} - bH \right] + \gamma_1 (H - H^*) (cP - d - lH) \\
&= (P - P^*) \left[ \frac{r(P - m_0)}{P + n_0} - \frac{r}{P + n_0} \frac{P}{K} (P - m_0) - bH - \frac{r(P^* - m_0)}{P^* + n_0} + bH^* \right. \\
&\quad \left. + \frac{r}{P^* + n_0} \frac{P^*}{K} (P^* - m_0) \right] + \frac{r}{P + n_0} \frac{P}{K} (P - m_0) (P - P^*) - \frac{r(P - m_0)}{P + n_0} \frac{P(t - \tau_1)}{K} (P - P^*) \\
&\quad + \gamma_1 (H - H^*) (cP - d - lH - cP^* + d + lH^*) \\
&= -(P - P^*)^2 \left[ \frac{r(m_0 n_0 - PP^* - n_0(P + P^*))}{K(n_0 + P^*)(n_0 + P)} - \frac{r(m_0 + n_0)}{(n_0 + P^*)(n_0 + P)} \right] \\
&\quad + \frac{r(P^* - m_0)}{K(P + n_0)} P(P - P^*) - \frac{r(P^* - m_0)}{K(P + n_0)} P(t - \tau_1)(P - P^*) - l\gamma_1 (H - H^*)^2 \\
&\quad - (b - c\gamma_1)(H - H^*)(P - P^*)
\end{aligned}$$

By setting  $\gamma_1 = \frac{b}{c}$ , the following result is derived

$$\begin{aligned}
\frac{dV_1}{dT} &= -(P - P^*) \left[ \frac{r(m_0 n_0 - PP^* - n_0(P + P^*))}{K(n_0 + P^*)(n_0 + P)} - \frac{r(m_0 + n_0)}{(n_0 + P^*)(n_0 + P)} \right] \\
&\quad + \frac{r(P^* - m_0)}{K(P + n_0)} P(P - P^*) - \frac{r(P^* - m_0)}{K(P + n_0)} P(t - \tau_1)(P - P^*) - l\gamma_1 (H - H^*)^2
\end{aligned}$$

Define  $V_2 = V_1 + \frac{r(P^* - m_0)P^*}{K(P + n_0)} \int_{t - \tau_1}^t \left( P(s) - P^* - P^* \ln \frac{P(s)}{P^*} \right) ds$  and then take its derivative.

$$\begin{aligned}
\frac{dV_2}{dT} &= \frac{dV_1}{dT} + \frac{r(P^* - m_0)P^*}{K(P + n_0)} \left[ P - P(t - \tau_1) - P^* \ln \left( \frac{P}{P(t - \tau_1)} \right) \right] \\
&\quad - (P - P^*)^2 \left[ \frac{r(m_0 n_0 - PP^* - n_0(P + P^*))}{K(n_0 + P^*)(n_0 + P)} - \frac{r(m_0 + n_0)}{(n_0 + P^*)(n_0 + P)} \right] \\
&\quad - \frac{lb}{c} (H - H^*)^2 + \frac{r(P^* - m_0)}{K(P + n_0)} P^2 - \frac{r(P^* - m_0)}{K(P + n_0)} P(t - \tau_1) P \\
&\quad + \frac{r(P^* - m_0)}{K(P + n_0)} (P^*)^2 \ln \left( \frac{P(t - \tau_1)}{P} \right)
\end{aligned}$$

Noting that  $\frac{r(P^*-m_0)}{K(P+n_0)}(P^*)^2 = \frac{r(P^*-m_0)}{K(P+n_0)}P^2$  at  $E_3(H^*, P^*)$ , we obtain

$$\begin{aligned} \frac{dV_2}{dT} = & -(P - P^*)^2 \left[ \frac{r(m_0n_0 - PP^* - n_0(P + P^*))}{K(n_0 + P^*)(n_0 + P)} - \frac{r(m_0 + n_0)}{(n_0 + P^*)(n_0 + P)} \right] \\ & - \frac{lb}{c}(H - H^*)^2 + \frac{r(P^* - m_0)}{K(P + n_0)}(P^*)^2 \left[ 1 - \frac{P}{P^*} \frac{P(t - \tau_1)}{P^*} + \ln \left( \frac{P(t - \tau_1)}{P} \right) \right] \end{aligned}$$

Therefore  $\frac{dV_2}{dT} < 0$  and the equality holds if and only if  $H = H^*$  and  $P = P^*$ . According to LaSalle's invariance principle, within the invariant set  $L = \{(H, P) \mid H = H^*, P = P^*\}$ , the equilibrium point  $E_3$  is globally asymptotically stable.  $\square$

### 3.2.2. Case with only gestation delay ( $\tau_1 = 0, \tau_2 > 0$ )

**Theorem 3.6.** *When  $\tau_1 = 0$  and  $\tau_2 > 0$ , under condition  $(W_1)$  in Theorem 2.6, the positive equilibrium point of system (1.3) is globally asymptotically stable.*

*Proof.* Define Lyapunov function  $V_3 = P - P^* - P^* \ln \left( \frac{P}{P^*} \right) + \gamma_2 \left( H - H^* - H^* \ln \frac{H}{H^*} \right)$  and  $\gamma_2$  is a normal number greater than zero. Differentiating the given expression yields

$$\begin{aligned} \frac{dV_3}{dT} = & \left( 1 - \frac{P^*}{P} \right) \frac{dP}{dT} + \gamma_2 \left( 1 - \frac{H^*}{H} \right) \frac{dH}{dT} \\ = & (P - P^*) \left[ \frac{r(P - m_0)}{P + n_0} \left( 1 - \frac{P}{K} \right) - bH \right] + \gamma_2 \left( 1 - \frac{H^*}{H} \right) [cP(t - \tau_2)H(t - \tau_2) - dH - lH^2] \\ = & (P - P^*) \left[ \frac{r(P - m_0)}{P + n_0} - \frac{r}{P + n_0} \frac{P}{K} (P - m_0) - bH - \frac{r(P^* - m_0)}{P^* + n_0} + bH^* \right. \\ & \left. + \frac{r}{P^* + n_0} \frac{P^*}{K} (P^* - m_0) \right] + \gamma_2 \left( 1 - \frac{H^*}{H} \right) [cP(t - \tau_2)H(t - \tau_2) - cP^*H^*] \\ & + \gamma_2 \left( 1 - \frac{H^*}{H} \right) [-d(H - H^*) - l(H - H^*)(H + H^*)] \\ = & -(P - P^*)^2 \left[ \frac{r(m_0n_0 - PP^* - n_0(P + P^*))}{K(n_0 + P^*)(n_0 + P)} - \frac{r(m_0 + n_0)}{(n_0 + P^*)(n_0 + P)} \right] \\ & - b(P - P^*)(H - H^*) + \gamma_2 \left( 1 - \frac{H^*}{H} \right) [cP(t - \tau_2)H(t - \tau_2) - cP^*H^*] \\ & - (H - H^*)^2 \frac{\gamma_2}{H} [l(H + H^*) + d] \end{aligned}$$

Define  $V_4 = V_3 + c\gamma_2 \int_{t-\tau_2}^t \left( P(s)H(s) - P^*H^* - P^*H^* \ln \frac{P(s)H(s)}{P^*H^*} \right) ds$  and then take its derivative.

$$\begin{aligned} \frac{dV_4}{dT} = & \frac{dV_3}{dT} + c\gamma_2 \left[ PH - P(t - \tau_2)H(t - \tau_2) - P^*H^* \ln \left( \frac{PH}{P(t - \tau_2)H(t - \tau_2)} \right) \right] \\ = & -(P - P^*)^2 \left[ \frac{r(m_0n_0 - PP^* - n_0(P + P^*))}{K(n_0 + P^*)(n_0 + P)} - \frac{r(m_0 + n_0)}{(n_0 + P^*)(n_0 + P)} \right] \\ & - b(P - P^*)(H - H^*) - (H - H^*)^2 \frac{\gamma_2}{H} [l(H + H^*) + d] + c\gamma_2 [P(H - H^*) + H^*(P - P^*)] \\ & + c\gamma_2 P^*H^* \left[ \frac{H^*}{H} - \frac{H^*}{H} \frac{P(t - \tau_2)H(t - \tau_2)}{P^*H^*} + \ln \frac{P(t - \tau_2)(H - \tau_2)}{PH} \right] \end{aligned}$$

Therefore  $\frac{dV_4}{dT} < 0$  and the equality holds if and only if  $H = H^*$  and  $P = P^*$ . According to LaSalle's invariance principle, within the invariant set  $L = \{(H, P) \mid H = H^*, P = P^*\}$ , the equilibrium point  $E_3$  is globally asymptotically stable.  $\square$

### 3.2.3. Case with both maturation delay and gestation delay ( $\tau_1 > 0, \tau_2 > 0$ )

**Theorem 3.7.** *When  $\tau_1 > 0$  and  $\tau_2 > 0$ , under condition  $(W_1)$  in Theorem 2.6, the positive equilibrium point of system (1.3) is globally asymptotically stable.*

*Proof.* Define Lyapunov function  $V_5 = P - P^* - P^* \ln\left(\frac{P}{P^*}\right) + \gamma_3 (H - H^* - H^* \ln\frac{H}{H^*})$  and  $\gamma_3$  is a normal number greater than zero. Differentiating the given expression yields

$$\begin{aligned} \frac{dV_5}{dT} &= \left(1 - \frac{P^*}{P}\right) \frac{dP}{dT} + \gamma_3 \left(1 - \frac{H^*}{H}\right) \frac{dH}{dT} \\ &= (P - P^*) \left[ \frac{r(P - m_0)}{P + n_0} - \frac{r(P - m_0)}{P + n_0} \cdot \frac{P(t - \tau_1)}{K} - bH \right] \\ &\quad + \gamma_3 \left(1 - \frac{H^*}{H}\right) [cP(t - \tau_2)H(t - \tau_2) - dH - lH^2] \\ &= -(P - P^*)^2 \left[ \frac{r(m_0 n_0 - PP^* - n_0(P + P^*))}{K(n_0 + P^*)(n_0 + P)} - \frac{r(m_0 + n_0)}{(n_0 + P^*)(n_0 + P)} \right] \\ &\quad - b(P - P^*)(H - H^*) + \frac{r(P^* - m_0)}{K(P + n_0)} P(P - P^*) - \frac{r(P^* - m_0)}{K(P + n_0)} P(t - \tau_1)(P - P^*) \\ &\quad + \gamma_3 \left(1 - \frac{H^*}{H}\right) [cP(t - \tau_2)H(t - \tau_2) - cP^*H^*] - \frac{\gamma_3}{H} (H - H^*)^2 [l(H + H^*) + d] \end{aligned}$$

We denote  $cH^*P^* = cH^*P$  at  $E_3(P^*, H^*)$ . Define  $V_6$  and then take its derivative.

$$\begin{aligned} V_6 &= V_5 + \frac{r(P^* - m_0)P^*}{K(P + n_0)} \int_{t-\tau_1}^t \left( P(s) - P^* - P^* \ln \frac{P(s)}{P^*} \right) ds \\ &\quad + c\gamma_3 \int_{t-\tau_2}^t \left( P(s)H(s) - P^*H^* - P^*H^* \ln \frac{P(s)H(s)}{P^*H^*} \right) ds \end{aligned}$$

$$\begin{aligned} \frac{dV_6}{dT} &= -(P - P^*)^2 \left[ \frac{r(m_0 n_0 - PP^* - n_0(P + P^*))}{K(n_0 + P^*)(n_0 + P)} - \frac{r(m_0 + n_0)}{(n_0 + P^*)(n_0 + P)} \right] \\ &\quad - b(P - P^*)(H - H^*) - (H - H^*)^2 \frac{\gamma_3}{H} [l(H + H^*) + d] \\ &\quad + \frac{r(P^* - m_0)}{K(P + n_0)} (P^*)^2 \left[ 1 - \frac{P}{P^*} \frac{P(t - \tau_1)}{P^*} + \ln \left( \frac{P(t - \tau_1)}{P} \right) \right] \\ &\quad + c\gamma_3 P^* H^* \left[ \frac{H^*}{H} - \frac{H^*}{H} \frac{P(t - \tau_2)H(t - \tau_2)}{P^*H^*} + \ln \left( \frac{P(t - \tau_2)(H - \tau_2)}{PH} \right) \right] \end{aligned}$$

Therefore  $\frac{dV_6}{dT} < 0$  and the equality holds if and only if  $H = H^*$  and  $P = P^*$ . According to LaSalle's invariance principle, within the invariant set  $L = \{(H, P) \mid H = H^*, P = P^*\}$ , the equilibrium point  $E_3$  is globally asymptotically stable.  $\square$

**Remark 3.8.** For the non-delay system (1.2), under condition  $(W_1)$  given in Theorem 2.6, the positive equilibrium is globally asymptotically stable. Under the same condition  $(W_1)$ , the positive equilibrium of the delay

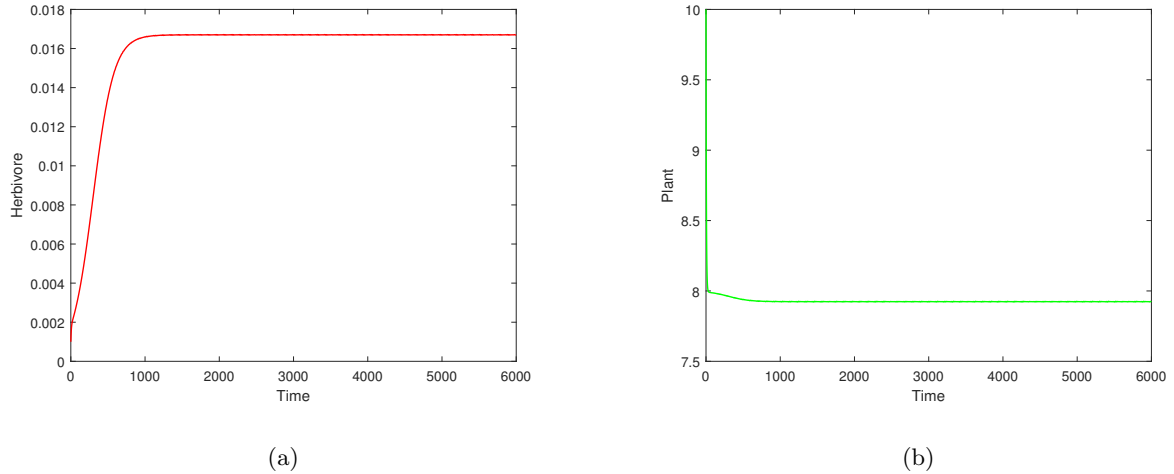


FIGURE 1. Figure (a) and figure (b) are time series plots of herbivores and plants respectively.

system (1.3) remains globally asymptotically stable, regardless of whether there is only a single delay or two delays in the system.

#### 4. NUMERICAL SIMULATIONS

In this section, the analytical predictions obtained in the preceding section will be verified by performing numerical simulations with MATLAB 2017b. We will investigate the regulatory mechanisms of time delay differences and Allee effect strength on the nonlinear oscillations, stability changes, and population dynamics of the plant–herbivore system, focusing on both non-delayed and delayed systems.

It should be noted that the parameter values used in the numerical simulations of this study are theoretical choices, satisfying the mathematical conditions required for stability and bifurcation analysis, rather than being derived from empirical data. Our aim is to illustrate the dynamical behaviors predicted by the model through numerical simulations and to explore the dynamical properties arising from the interaction between double Allee effect and double time delay, rather than to make quantitative predictions for a specific plant–herbivore system.

##### 4.1. Non-delayed system

For the model (1.2) we select the following dataset, which satisfies the three conditions outlined in Theorem 2.6

$$\begin{aligned} r = 0.2, \quad K = 8.8, \quad n_0 = 1, \quad m_0 = 0.1, \\ b = 0.1, \quad c = 0.059, \quad d = 0.465, \quad l = 0.15. \end{aligned} \quad (4.1)$$

Meanwhile, the initial condition is  $P(0) = 10$ ,  $H(0) = 0.001$  and the value of the equilibrium point is  $E_3(0.16699, 7.92381)$ .

From Figure 1a and 1b, it can be observed that the population density of the herbivore initially increases before stabilizing, while the population density of the plant initially decreases and subsequently reaches a stable level. Furthermore, 2a demonstrates the absence of closed orbits in the system. These results collectively indicate that the equilibrium point  $E_3$  is globally stable.

Figure 2b is the phase portrait under multiple sets of initial values, with initial values of  $(7,1)$ ,  $(10,0.5)$ ,  $(10,0.2)$ ,  $(10,1)$  respectively. By analyzing the solution curves under different initial values, we find that as long as the model parameters meet the conditions of the existence and stability of the equilibrium point, the change of the initial value will not change the position of the equilibrium point. All trajectories eventually tend to the

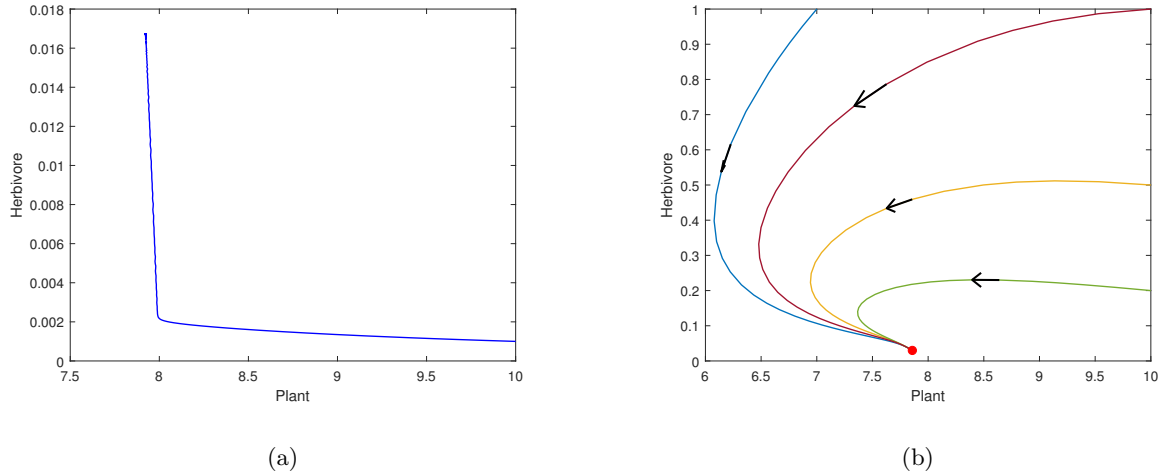


FIGURE 2. Figure (a) illustrates the time series plot, while Figure (b) depicts the solution curves under varying initial conditions.

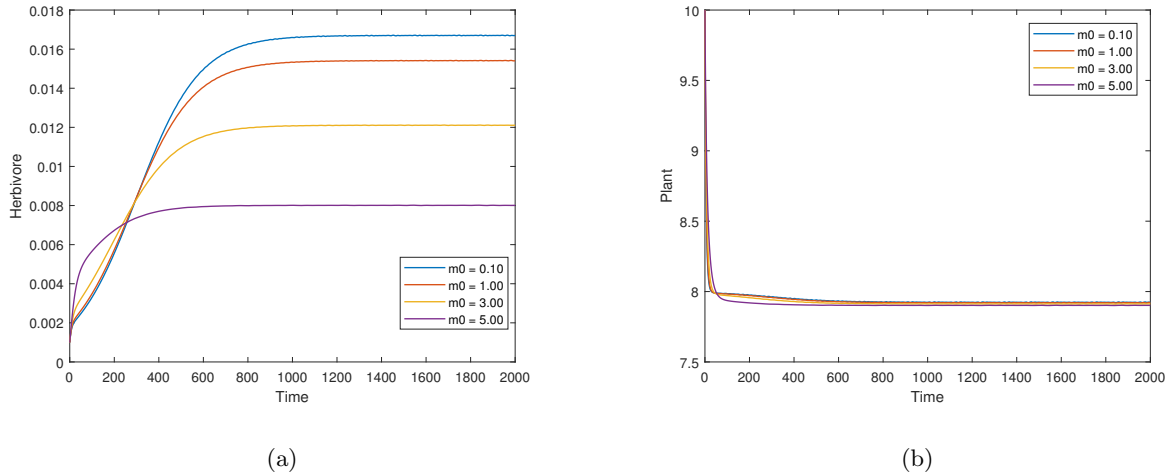


FIGURE 3. Figures (a) and (b) depict the time series plots of the plant and herbivore populations for varying initial values of  $m_0$ .

same equilibrium point, which shows that the long-term behavior of the system is determined by parameters, and the initial value only affects the path and convergence speed of the trajectory. This conclusion is consistent with the classical ecological theory and further verifies the stability of the the plant–herbivore model [27, 28].

Figure 3a and Figure 3b illustrate the influence of the Allee effect parameter  $m_0$  on the dynamics of herbivore and plant populations. The results demonstrate that as the value of  $m_0$  increases, the plant population size decreases, while the herbivore population size exhibits an upward trend. This finding confirms that  $m_0$ , as a critical indicator of the Allee effect intensity, plays a significant role in modulating the interaction between plants and herbivores, thereby exerting a profound impact on the population dynamics of both species.

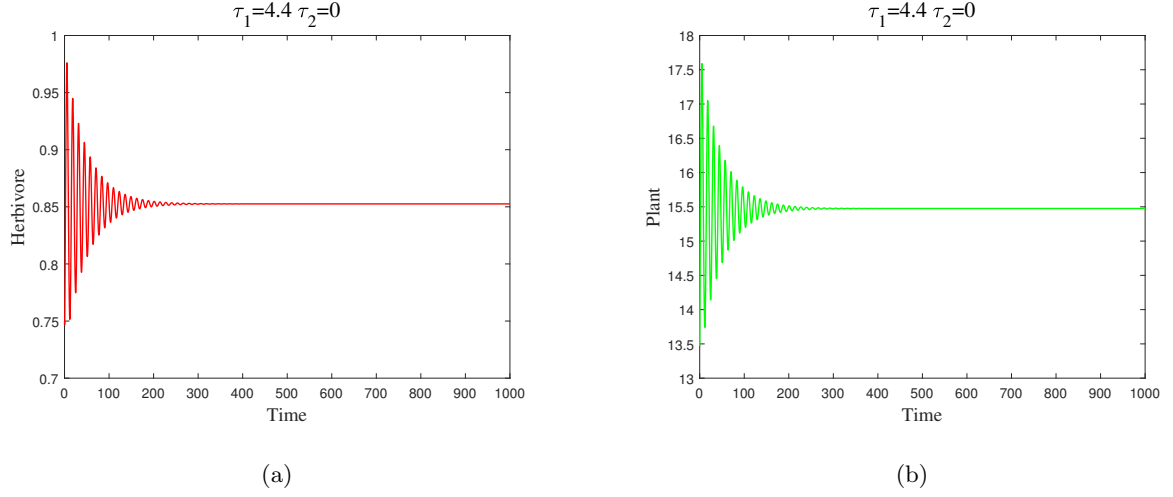


FIGURE 4. Figure (a) and figure (b) are time series plots of herbivores and plants respectively.

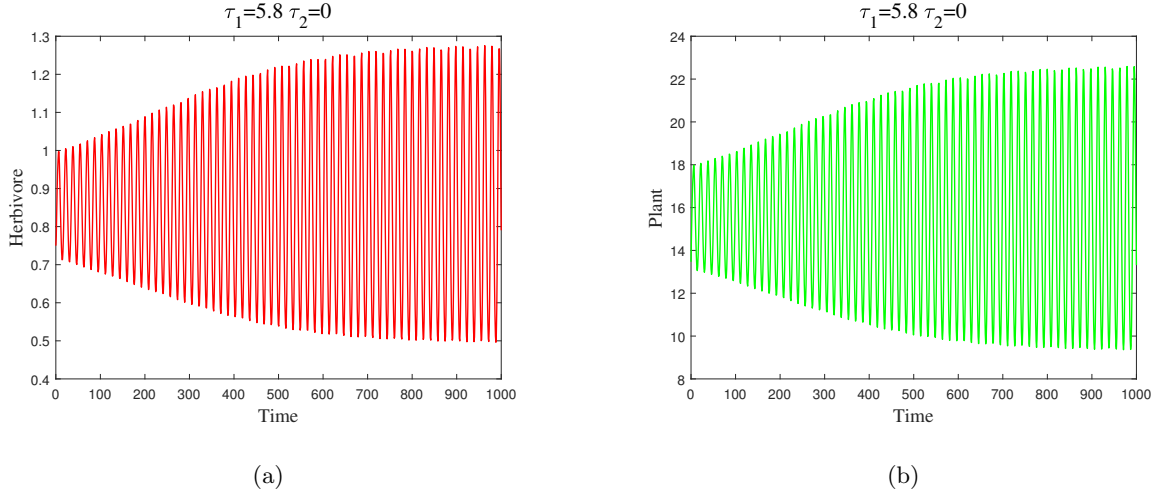


FIGURE 5. Figure (a) and figure (b) are time series plots of herbivores and plants respectively.

## 4.2. Delayed system

Next, we will explore the effects of time delay differences and Allee effect strength on the stability changes and population dynamics of the plant–herbivore system from the perspective of time-delayed systems.

Case(I): When  $\tau_1 > 0$ ,  $\tau_2 = 0$ , we select the following datas

$$\begin{aligned} r &= 0.85, & K &= 26, & n_0 &= 1.1, & m_0 &= 1.1, \\ b &= 0.35, & c &= 0.15, & d &= 0.19, & l &= 2.5. \end{aligned} \quad (4.2)$$

Through calculation, the value of the equilibrium point is  $E_3(0.85255, 15.47588)$ , and there are  $\omega_1 = 0.404611$ ,  $\tau_1^0 = 5.52790$ .

Figure 4 illustrates the population dynamics of herbivores and plants over time when  $\tau_1 = 4.4$ . As shown in the figure, the population densities of both species eventually converge to stable values, indicating that the

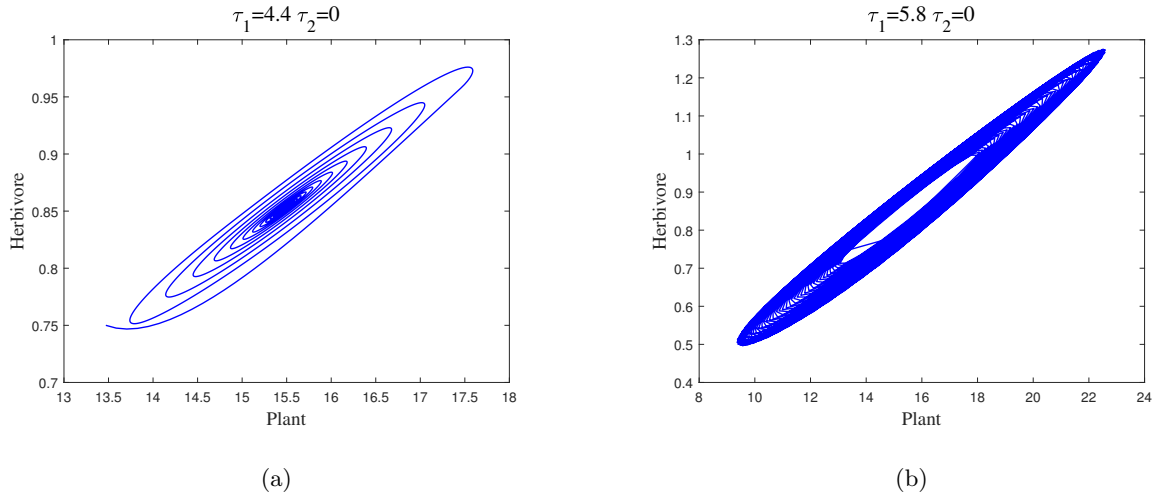


FIGURE 6. Figures (a) and figure (b) are phase portraits of herbivores and plants respectively.

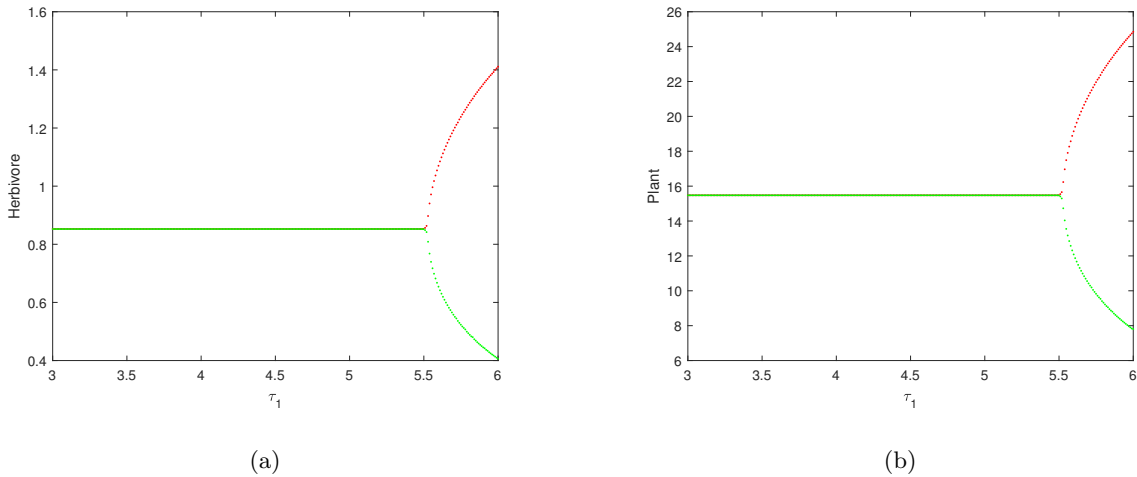


FIGURE 7. Figures (a) and (b) present the bifurcation diagrams of herbivore and plant populations, respectively, with respect to the maturation delay  $\tau_1$ , when  $\tau_2 = 0$ .

equilibrium point  $E_3$  is locally asymptotically stable under these conditions. However, when  $\tau_1$  is increased to 5.8 as depicted in Figure 5, exceeding the critical delay threshold, the population densities of herbivores and plants exhibit persistent instability, characterized by oscillatory behavior.

Furthermore, Figure 6 reveals the formation of a limit cycle near the equilibrium point  $E_3$ , demonstrating that the equilibrium point  $E_3$  becomes unstable under this parameter configuration. These results collectively demonstrate that as the time delay parameter  $\tau_1$  increases, the system's dynamic behavior transitions from stability to instability, highlighting the significant influence of time delay on the stability of the ecosystem.

Figure 7 shows the bifurcation diagram with  $\tau_1$  as the bifurcation parameter. When the delay surpasses the critical threshold, the system undergoes a transition from a stable to an unstable state *via* a Hopf bifurcation.

Case(II): When  $\tau_2 > 0, \tau_1 \in [0, \tau_1^0)$ , the parameter selection is the same as (4.2). We choose  $\tau_1 = 3 \in [0, 5.52790)$ . Through calculation, the value of the equilibrium point is  $E_3(0.85255, 15.47588)$ , and there are  $\omega_4 = 0.6212, \tau_{2*}^0 = 0.525365$ .

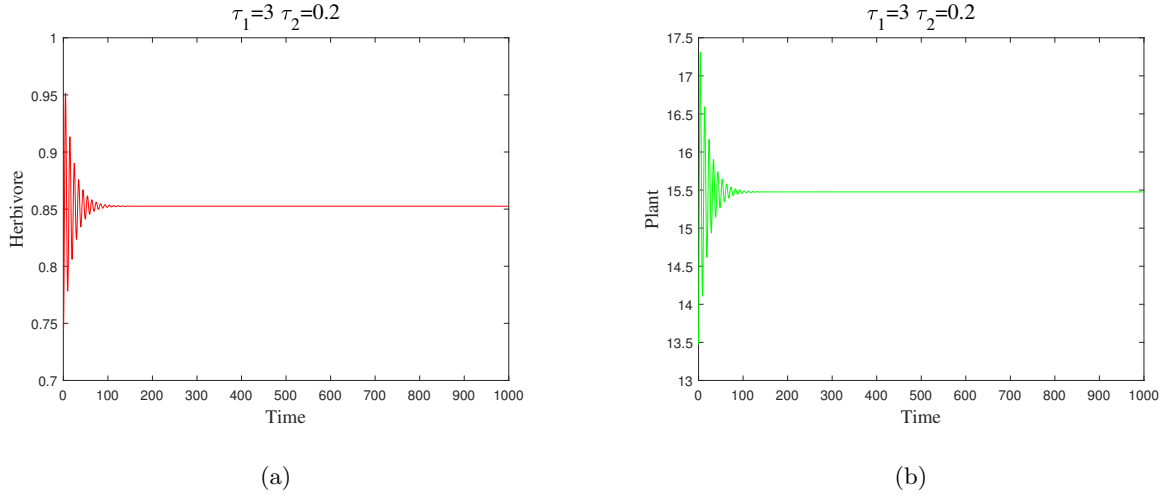


FIGURE 8. Figure (a) and figure (b) are time series plots of herbivores and plants respectively.

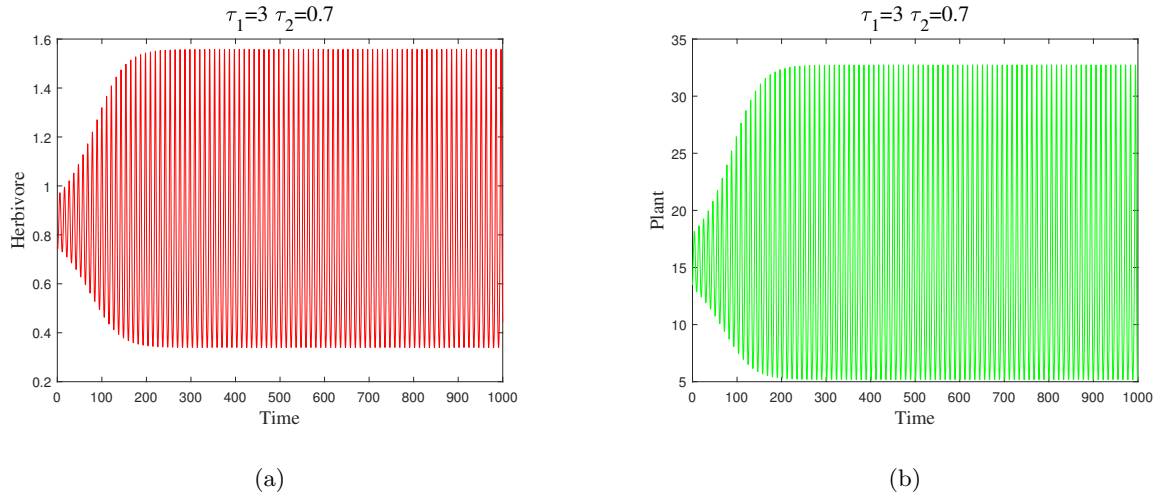


FIGURE 9. Figure (a) and figure (b) are time series plots of herbivores and plants respectively.

Figure 8 demonstrates that when  $\tau_2 = 0.2$  and  $\tau_1 = 3 \in [0, 5.52790)$ , the population densities of herbivores and plants eventually stabilize, indicating that the equilibrium point  $E_3$  is locally asymptotically stable. However, Figure 9 reveals that when  $\tau_2 = 0.7$ , exceeding the critical delay threshold, the population densities of both species become unstable and exhibit persistent oscillations. Furthermore, Figure 10b reveals the formation of a limit cycle near the equilibrium point  $E_3$  demonstrating that  $E_3$  is unstable under these conditions.

Figure 11 shows the bifurcation diagram with  $\tau_2$  as the bifurcation parameter. When the delay surpasses the critical threshold, the system undergoes a transition from a stable to an unstable state *via* a Hopf bifurcation.

Figure 12a demonstrates the relationship between parameter  $m_0$  and the critical time delay  $\tau_{2*}$ . The results indicate that the stable region lies below the curve, while the unstable region is above it, with  $\tau_{2*}$  showing a monotonic decrease as  $m_0$  increases. This reveals that system stability is coregulated by  $m_0$  and  $\tau_{2*}$ , where larger  $m_0$  values tend to destabilize the system, demonstrating the negative regulatory effect of the Allee effect on system stability. Figure 12b illustrates the influence of the Allee effect parameter  $m_0$  on plant population

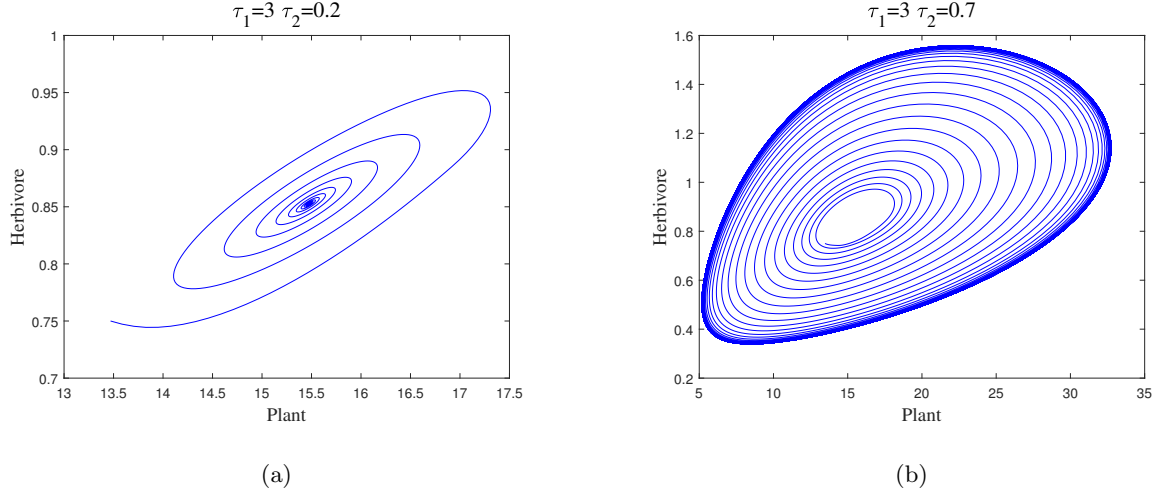


FIGURE 10. Figures (a) and figure (b) are phase portraits of herbivores and plants respectively.

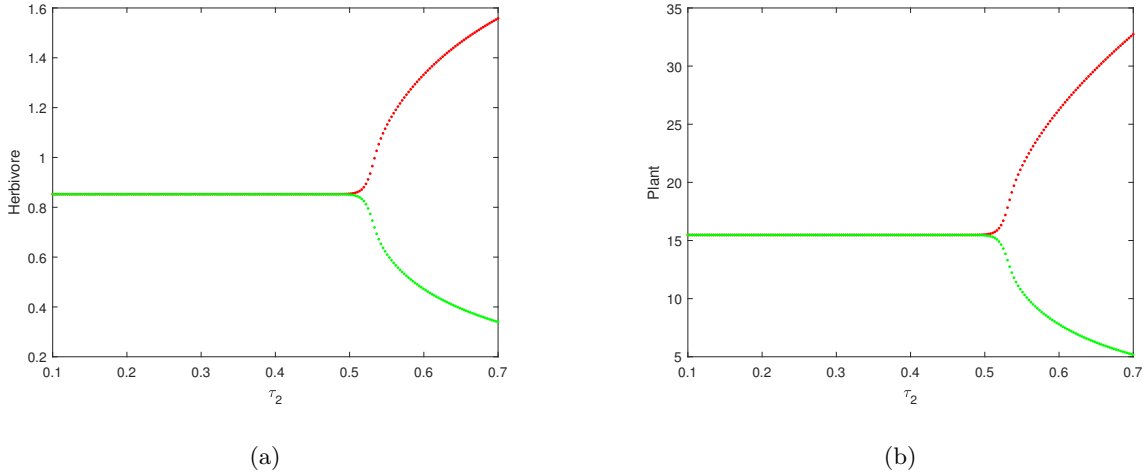


FIGURE 11. Figures (a) and (b) present the bifurcation diagrams of herbivore and plant populations, respectively, with respect to the gestation delay  $\tau_2$ , when  $\tau_1 = 3$ .

dynamics. The results demonstrate that population size decreases with increasing  $m_0$  values, confirming that  $m_0$ , as an indicator of Allee effect intensity, significantly influences plant population abundance.

Case(III): When  $\tau_1 = 0$ ,  $\tau_2 > 0$ , we select the following datas

$$\begin{aligned} r &= 0.65, & K &= 20, & n_0 &= 0.5, & m_0 &= 0.5, \\ b &= 0.1, & c &= 0.13, & d &= 0.2, & l &= 0.15. \end{aligned} \quad (4.3)$$

Through calculation, the value of the equilibrium point is  $E_3(3.85267, 5.98387)$ , and there are  $\omega_2 = 0.15668$ ,  $\tau_2^0 = 9.70454$ .

Figure 13 illustrates the population dynamics of herbivores and plants over time when  $\tau_2 = 8.2$ . As shown in the figure, the population densities of both species eventually converge to stable values, indicating that the equilibrium point  $E_3$  is locally asymptotically stable under these conditions. However, when  $\tau_2$  is increased to

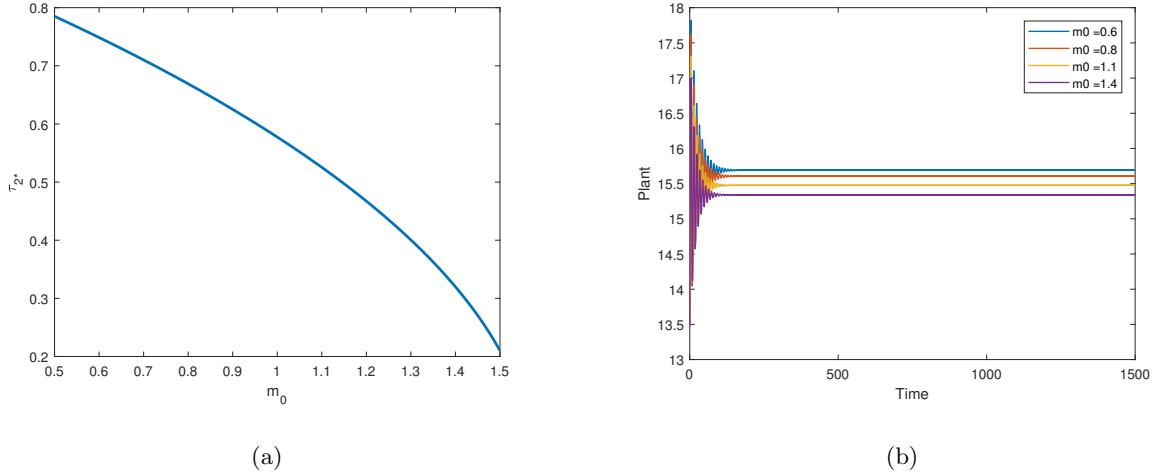


FIGURE 12. Figures (a) is bifurcation diagram of the critical delay value with respect to the parameter  $m_0$ , where  $\tau_2 = 0.2$ ,  $\tau_1 = 3$ . Figures (b) presents the time series plots of the plant population across varying initial  $m_0$  values, where  $\tau_2 = 0.2$ ,  $\tau_1 = 3$ .

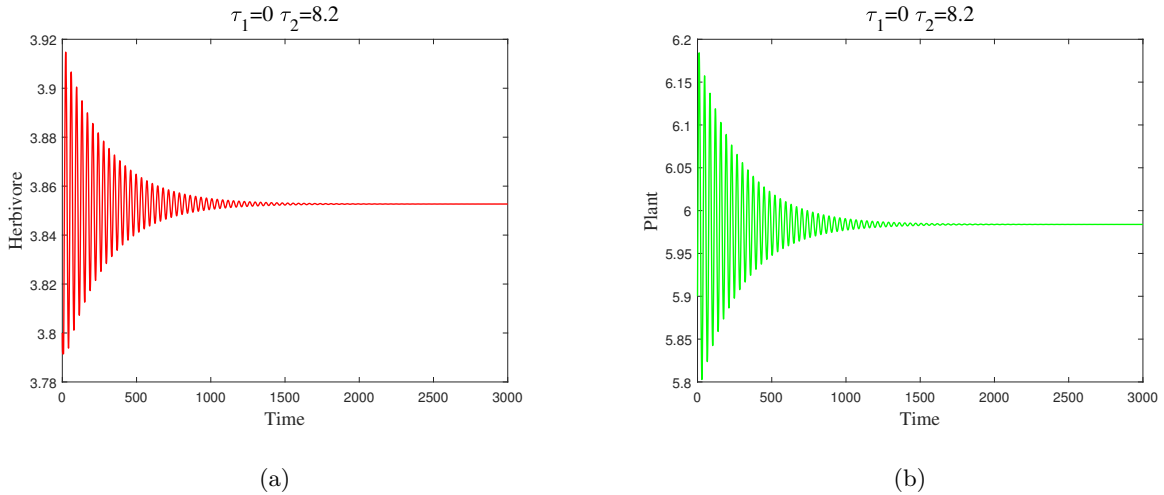


FIGURE 13. Figure (a) and figure (b) are time series plots of herbivores and plants respectively.

11 as depicted in Figure 14, exceeding the critical delay threshold, the population densities of herbivores and plants exhibit persistent instability, characterized by oscillatory behavior.

Furthermore, Figure 15b reveals the formation of a limit cycle near the equilibrium point  $E_3$ , demonstrating that the equilibrium point  $E_3$  becomes unstable under this parameter configuration. These results collectively demonstrate that as the time delay parameter  $\tau_2$  increases, the system's dynamic behavior transitions from stability to instability, highlighting the significant influence of time delay on the stability of the ecosystem.

Figure 16 shows the bifurcation diagram with  $\tau_2$  as the bifurcation parameter. When the delay surpasses the critical threshold, the system undergoes a transition from a stable to an unstable state *via* a Hopf bifurcation.

Case(IV): When  $\tau_1 > 0, \tau_2 \in [0, \tau_2^0)$ , the parameter selection is the same as (4.3). We choose  $\tau_2 = 8.2 \in [0, 9.70454)$ . Through calculation, the value of the equilibrium point is  $E_3(3.85267, 5.98387)$ , and there are  $\omega_3 = 0.18127, \tau_{1*}^0 = 0.75832$ .

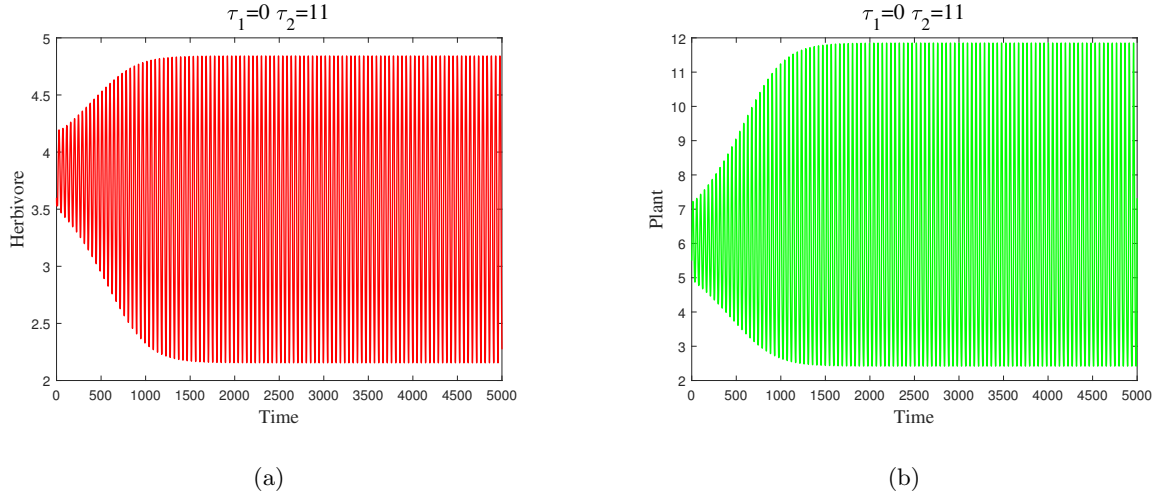


FIGURE 14. Figure (a) and figure (b) are time series plots of herbivores and plants respectively.

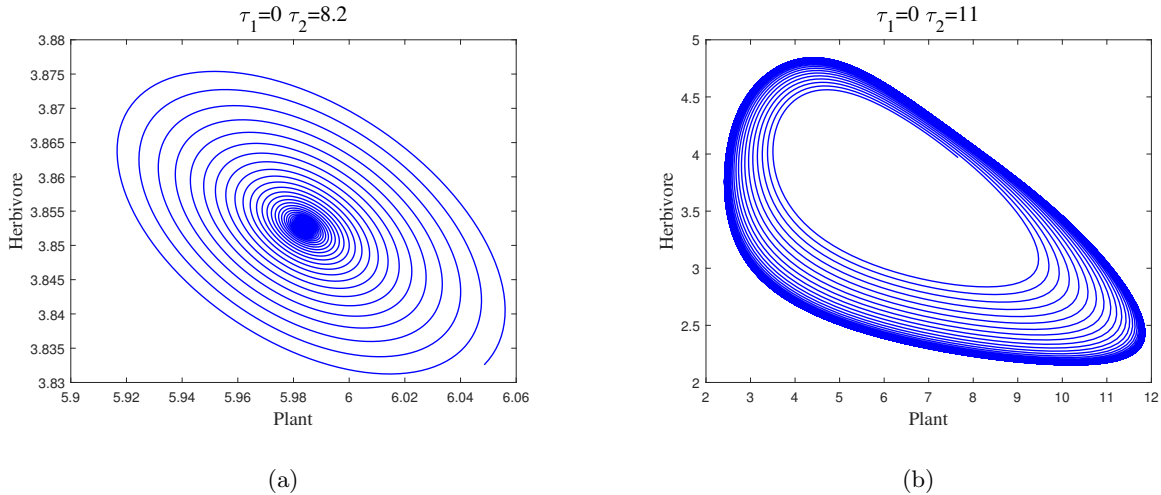


FIGURE 15. Figure (a) and figure (b) are phase portraits of herbivores and plants respectively.

Figure 17 demonstrates that when  $\tau_1 = 0.3$  and  $\tau_2 = 8.2 \in [0, 9.70454)$ , the population densities of herbivores and plants eventually stabilize, indicating that the equilibrium point  $E_3$  is locally asymptotically stable. However, Figure 18 reveals that when  $\tau_1 = 1.3$ , exceeding the critical delay threshold, the population densities of both species become unstable and exhibit persistent oscillations. Furthermore, Figure 19b reveals the formation of a limit cycle near the equilibrium point  $E_3$  demonstrating that  $E_3$  is unstable under these conditions.

Figure 20 shows the bifurcation diagram with  $\tau_1$  as the bifurcation parameter. When the delay surpasses the critical threshold, the system undergoes a transition from a stable to an unstable state *via* a Hopf bifurcation.

Figure 21a demonstrates the quantitative relationship between parameter  $m_0$  and the critical time delay  $\tau_{1*}$ . The stability region is observed below the curve, while the instability region lies above it. Quantitative analysis reveals that the critical time delay  $\tau_{1*}$  exhibits a monotonically decreasing trend with increasing  $m_0$ . This phenomenon indicates that the stability characteristics of the system are significantly dependent on the coupling effect between  $m_0$  and time delay  $\tau_{1*}$ . Specifically, when  $m_0$  takes larger values, the system becomes

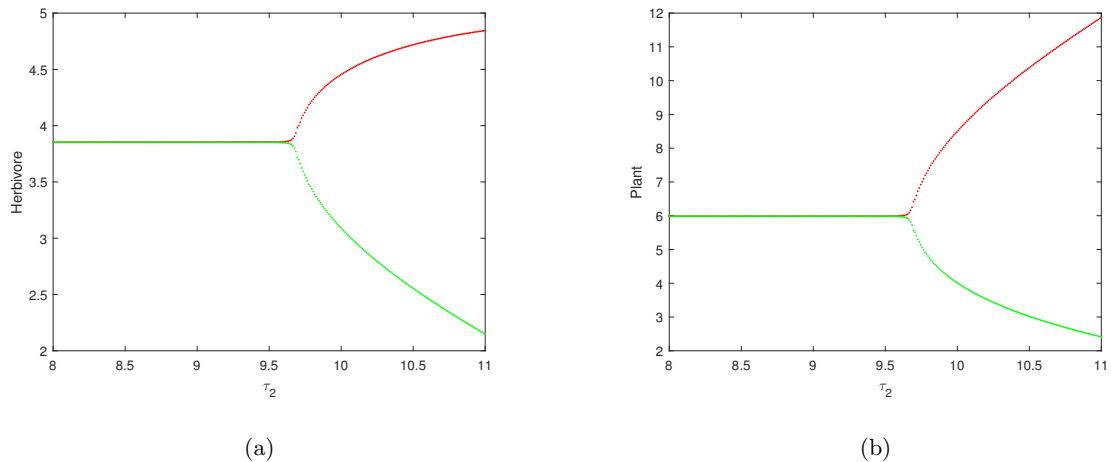


FIGURE 16. Figures (a) and (b) present the bifurcation diagrams of herbivore and plant populations, respectively, with respect to the gestation delay  $\tau_2$ , when  $\tau_1 = 0$ .

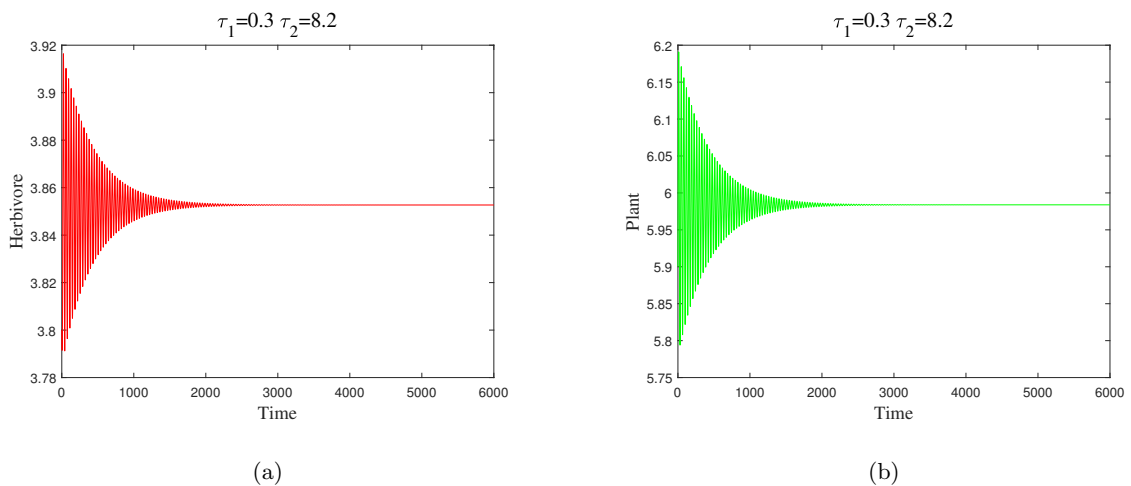


FIGURE 17. Figure (a) and figure (b) are time series plots of herbivores and plants respectively.

more prone to instability, which reveals that the Allee effect exerts a significant destabilizing regulatory influence on the system stability in this model, demonstrating a tendency to drive the system towards instability.

Figure 21b illustrates the impact of the Allee effect parameter  $m_0$  on plant population dynamics. The results demonstrate that population size decreases with increasing  $m_0$  values, confirming that  $m_0$ , as an indicator of Allee effect intensity, significantly influences plant population abundance.

## 5. CONCLUSION

In this paper, we deeply explored a generalized plant–herbivore model by innovatively incorporating two distinct discrete delays: a maturation delay in the plant trophic level and a gestation delay in herbivores. Within the Holling I functional response framework, the model integrates double Allee effects in the plant trophic level and introduces an intraspecific competition term for herbivores, significantly enhancing its capacity to characterize realistic ecological interactions.

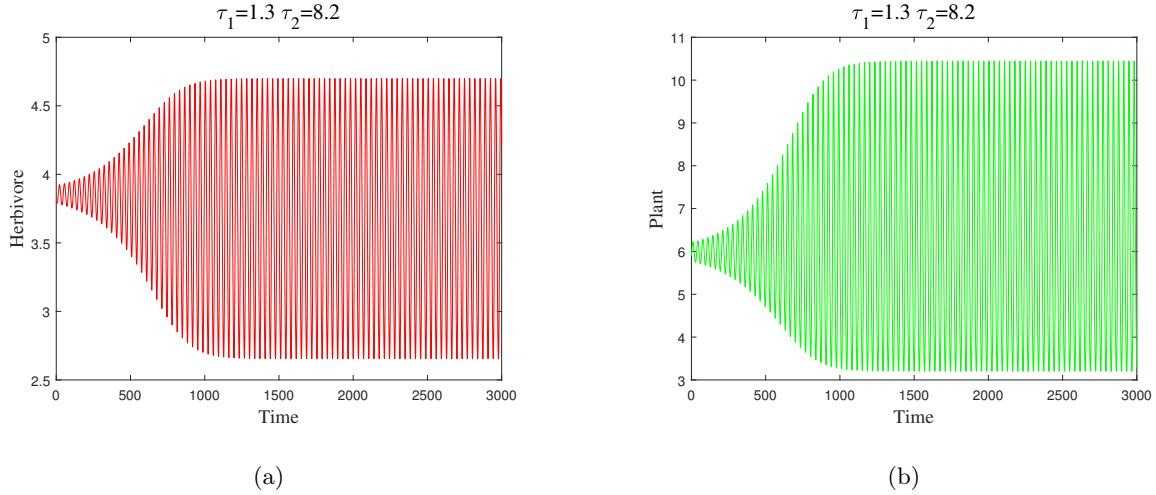


FIGURE 18. Figure (a) and figure (b) are time series plots of herbivores and plants respectively.

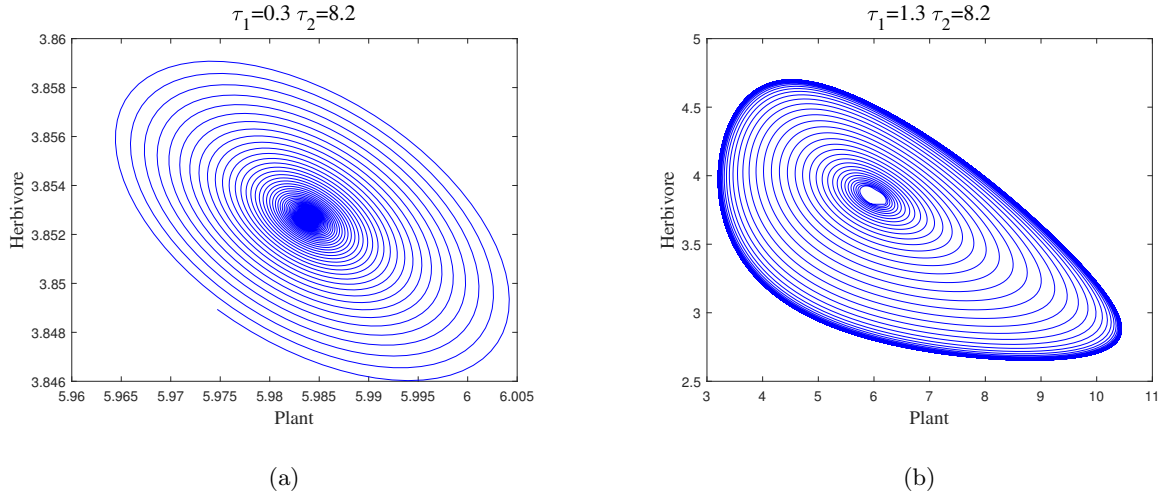


FIGURE 19. Figure (a) and figure (b) are phase portraits of herbivores and plants respectively.

Through rigorous theoretical analysis, we systematically establish the existence conditions for positive equilibria and demonstrate solution boundedness, thereby providing a robust mathematical foundation that ensures the model’s applicability to real ecological scenarios. Detailed examinations are conducted on the local stability and Hopf bifurcation of trivial equilibrium, boundary equilibrium, and positive equilibrium in the non-delayed system, complemented by an exploration of global stability under specific conditions. Furthermore, we comprehensively analyze the existence of Hopf bifurcations under four combination scenarios of double delays and investigate global stability under three delay combinations.

Numerical simulations reveal that time delays exert destabilizing effects on system stability. When delays exceed critical threshold values, the system undergoes Hopf bifurcation, transitioning from stable to unstable states. Notably, the Allee effects significantly modulate the impact of delays, manifested by a monotonic decrease in critical delay thresholds as the Allee intensity parameter  $m_0$  increases, thereby rendering the system more susceptible to instability. This finding profoundly reveals that the stability characteristics of the system

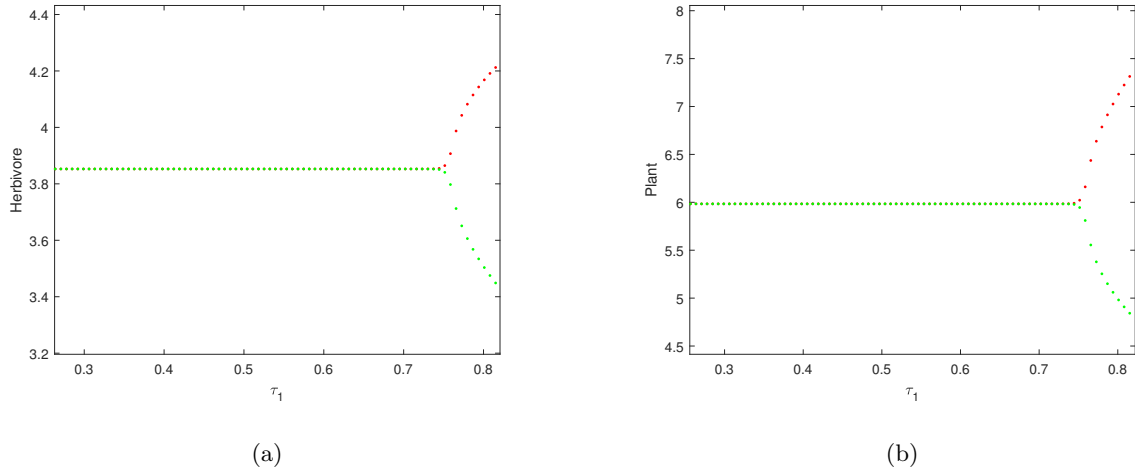


FIGURE 20. Figures (a) and (b) present the bifurcation diagrams of herbivore and plant populations, respectively, with respect to the maturation delay  $\tau_1$ , when  $\tau_2 = 8.2$ .

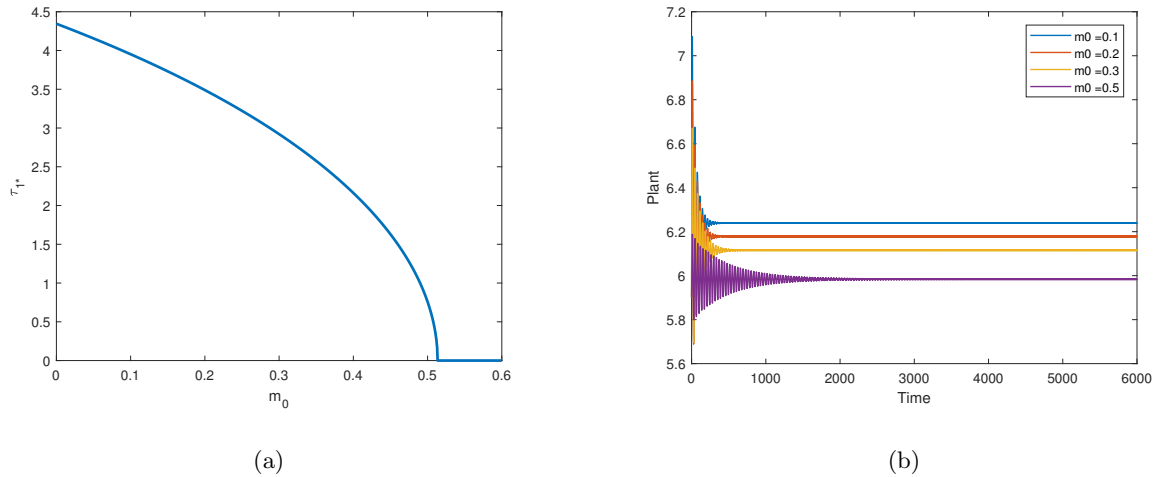


FIGURE 21. Figures (a) is bifurcation diagram of the critical delay value with respect to the parameter  $m_0$ , where  $\tau_1 = 0.3$ . Figures (b) presents the time series plots of the plant population across varying initial  $m_0$  values, where  $\tau_1 = 0.3$ ,  $\tau_2 = 8.2$ .

significantly depend on the coupling relationship between the double Allee effects and time delay, highlighting that the double Allee effect has a significant negative regulatory effect on the stability of the system in this model. Moreover, we also found that the intensity of the double Allee effect has a significant impact on the plant population size. As the value of the Allee effect intensity index  $m_0$  increases, the population size decreases.

Compared with classical plant–herbivore models incorporating time delays and Allee effects [17–22], this study reveals several distinctive features. First, existing single-delay models [23, 24] indicate that increasing intraspecific competition contributes to system stability; however, our dual-delay framework shows that the critical delay threshold is highly sensitive to the type of delay and the strength of the Allee effect. This synergistic destabilization cannot be explained by single-delay models. Second, although previous studies [17–22] have typically treated the Allee effect as an independent factor, our analysis demonstrates a nonlinear interaction between the double Allee effect and time delays, with the critical delay threshold monotonically decreasing as

the Allee strength  $m_0$  increases. Furthermore, we find that the same delay can either stabilize or destabilize the system, depending on the presence of the other delay and the position of the population density relative to the Allee threshold. This finding has important implications for conservation biology, suggesting that management strategies should consider the interactive effects of multiple delays and Allee effects comprehensively, rather than addressing them separately.

From an ecological perspective, the interaction between double delays and double Allee effects exhibits distinct regulatory patterns under different delay combinations. In the case of only maturation delay ( $\tau_1 > 0, \tau_2 = 0$ ), the Allee effect primarily influences plant recruitment dynamics. When plant density falls below the Allee threshold, population recovery slows down, thereby amplifying the destabilizing effect caused by the delay. In the case of only gestation delay ( $\tau_1 = 0, \tau_2 > 0$ ), the Allee effect indirectly affects herbivore reproduction through plant abundance. Lower plant density exacerbates the impact of reproductive delay, making the population more prone to extinction. When both delays are present ( $\tau_1 > 0, \tau_2 > 0$ ), a synergistic destabilizing effect emerges. The maturation delay weakens plant regeneration capacity, while the gestation delay separates herbivore consumption from reproduction in time. The double Allee effect further intensifies this synergy by reducing the population growth rate at low densities, making the system more susceptible to oscillations or even collapse. These findings indicate that the ecological consequences of time delays are not fixed, but are critically influenced by the presence and intensity of Allee effects at different trophic levels.

Further analysis of how delay duration affects the system reveals that the coupling between Allee effects and delays also depends on population density. When the maturation delay ( $\tau_1$ ) increases, plants respond more slowly to resource consumption, making recovery more difficult at low densities. When the gestation delay ( $\tau_2$ ) increases, herbivores respond with a lag to food availability changes, making them more likely to miss breeding opportunities at low densities. The lower the population density, the more pronounced the decline in per-capita growth rate. Consequently, when density approaches the Allee threshold, the system becomes more sensitive to delays, and even small delays may trigger instability. When density is well above the threshold, the system can tolerate larger delays (Fig. 21a). This finding suggests that special attention should be paid to time delay factors in the conservation of low-density populations.

This study enriches the theoretical system of ecological models with double time delays and double Allee effects, providing new ideas and methods for analyzing the dynamic behavior of complex ecological systems. In terms of practical applications, the research results of this paper have important practical significance. For ecological protection, clarifying the impacts of the double Allee effect and double time delays on the stability of the system and population size helps us formulate more targeted conservation strategies to avoid species extinction due to system instability or excessive decline in population size. In ecosystem management, it can provide a scientific basis for rational resource planning and maintaining ecological balance, contributing to the realization of the sustainable development of the ecosystem. It is worth noting that the parameter values used in the numerical simulations of this study are theoretical choices, aimed at demonstrating the dynamical behaviors predicted by the model. In future work, we will obtain empirical data from actual plant-herbivore systems to calibrate the model parameters and validate the theoretical findings in a real ecological context, thereby enhancing the practical applicability of the model in conservation and ecosystem management.

#### ACKNOWLEDGMENTS

We would like to express our sincere gratitude to all the teachers and classmates who have contributed to this paper. We are also deeply thankful to the reviewers for their valuable comments and suggestions, which have significantly improved the quality of our work.

#### REFERENCES

- [1] A.J. Lotka, Undamped oscillations derived from the law of mass action. *J. Am. Chem. Soc.* **42** (1920) 1595–1599.
- [2] V. Volterra, Fluctuations in the abundance of a species considered mathematically. *Nature* **119** (1927) 12–13.
- [3] R. Liu, Z. Feng, H. Zhu *et al.*, Bifurcation analysis of a plant-herbivore model with toxin-determined functional response. *J. Differ. Equ.* **245** (2008) 442–467.

- [4] Z. Huang, Q. Li and J. Cao, Dynamics in a stochastic diffusive plant–herbivore system. *Chaos Solitons Fractals* **151** (2021) 111147.
- [5] M.D. Asfaw, S.M. Kassa and E.M. Lungu, Stochastic plant–herbivore interaction model with Allee effect. *J. Math. Biol.* **79** (2019) 2183–2209.
- [6] V. Castellanos and F. Sánchez-Garduño, The existence of a limit cycle in a pollinator–plant–herbivore mathematical model. *Nonlinear Anal. Real World Appl.* **48** (2019) 212–231.
- [7] M.D. Asfaw, S.M. Kassa, E.M. Lungu *et al.*, Effects of temperature and rainfall in plant–herbivore interactions at different altitude. *Ecol. Model.* **406** (2019) 50–59.
- [8] W.C. Allee, Animal aggregations. *Quart. Rev. Biol.* **2** (1927) 367–398.
- [9] E. Beso, S. Kalabusic and E. Pilav, Dynamics of a plant–herbivore system with Ricker plant growth and the strong Allee effects on plant population. *Discrete Continuous Dyn. Syst. B* **29** (2024) 627–665.
- [10] M.D. Asfaw, S.M. Kassa and E.M. Lungu, Co-existence thresholds in the dynamics of the plant–herbivore interaction with Allee effect and harvest. *Int. J. Biomath.* **11** (2018) 1850057.
- [11] P.J. Pal and R. Saha, Qualitative analysis of a predator–prey system with double Allee effect in prey. *Chaos Solitons Fractals* **73** (2015) 36–63.
- [12] F. Wang, R. Yang and X. Zhang, Turing patterns in a predator–prey model with double Allee effect. *Math. Comput. Simul.* **220** (2024) 170–191.
- [13] J. Jiao and C. Chen, Bogdanov–Takens bifurcation analysis of a delayed predator–prey system with double Allee effect. *Nonlinear Dyn.* **104** (2021) 1697–1707.
- [14] D.S. Boukal and L. Berec, Single-species models of the Allee effect: extinction boundaries, sex ratios and mate encounters. *J. Theor. Biol.* **218** (2002) 375–394.
- [15] Z. Shang and Y. Qiao, Multiple bifurcations in a predator–prey system of modified Holling and Leslie type with double Allee effect and nonlinear harvesting. *Math. Comput. Simul.* **205** (2023) 745–764.
- [16] M.K. Singh, B.S. Bhadauria and B.K. Singh, Bifurcation analysis of modified Leslie–Gower predator–prey model with double Allee effect. *Ain Shams Eng. J.* **9** (2018) 1263–1277.
- [17] P.J. Pal, P.K. Mandal and K.K. Lahiri, A delayed ratio-dependent predator–prey model of interacting populations with Holling type III functional response. *Nonlinear Dyn.* **76** (2014) 201–220.
- [18] Y. Enatsu, J. Roy and M. Banerjee, Hunting cooperation in a prey–predator model with maturation delay. *J. Biol. Dyn.* **18** (2024) 2332279.
- [19] S.A. Gourley and Y. Kuang, A stage structured predator–prey model and its dependence on maturation delay and death rate. *J. Math. Biol.* **49** (2004) 188–200.
- [20] R.K. Upadhyay and D. Barman, Deciphering two delay dynamics of ecological system with generalist predator incorporating competitive interference. *Physica D: Nonlinear Phenomena* **468** (2024) 134293.
- [21] A. Kumar and B. Dubey, Modeling the effect of fear in a prey–predator system with prey refuge and gestation delay. *Int. J. Bifurcat. Chaos* **29** (2019) 1950195.
- [22] L. Deng, X. Wang and M. Peng, Hopf bifurcation analysis for a ratio-dependent predator–prey system with two delays and stage structure for the predator. *Appl. Math. Computat.* **231** (2014) 214–230.
- [23] P. Kumar and R. Verma, A delayed plant–herbivore model with a strong Allee effect in plant population. *Eur. Chem. Bull.* **12** (2023) 174–183.
- [24] P. Kumar and R. Verma, The study of stability analysis of modified Leslie–Gower herbivore Model with Allee effect in plants. *Contemp. Math.* (2024) 284–295.
- [25] S. Winggins, Introduction to Applied Nonlinear Dynamical Systems and Chaos. Springer New York, New York, NY (2003).
- [26] B. Dubey, A. Kumar and A.P. Maiti, Global stability and Hopf-bifurcation of prey–predator system with two discrete delays including habitat complexity and prey refuge. *Commun. Nonlinear Sci. Numer. Simul.* **67** (2019) 528–554.
- [27] J.D. Murray, Mathematical Biology I: An Introduction. Springer (2002).
- [28] M. Kot, Elements of Mathematical Ecology. Cambridge University Press (2001).